Different methods to derive the mixing-layer height by remote sensing (including RASS)

Stefan Emeis
Institute for Meteorology and Climate Research
Atmospheric Environmental Research Division (IMK-IFU)
Forschungszentrum Karlsruhe GmbH
Kreuzeckbahnstr. 19
82467 Garmisch-Partenkirchen, Germany
E-mail: stefan.emeis@kit.edu

Introduction

- relevance for wind energy

- definition of mixing layer

-remote sensing

Diurnal variation of vertical wind profiles

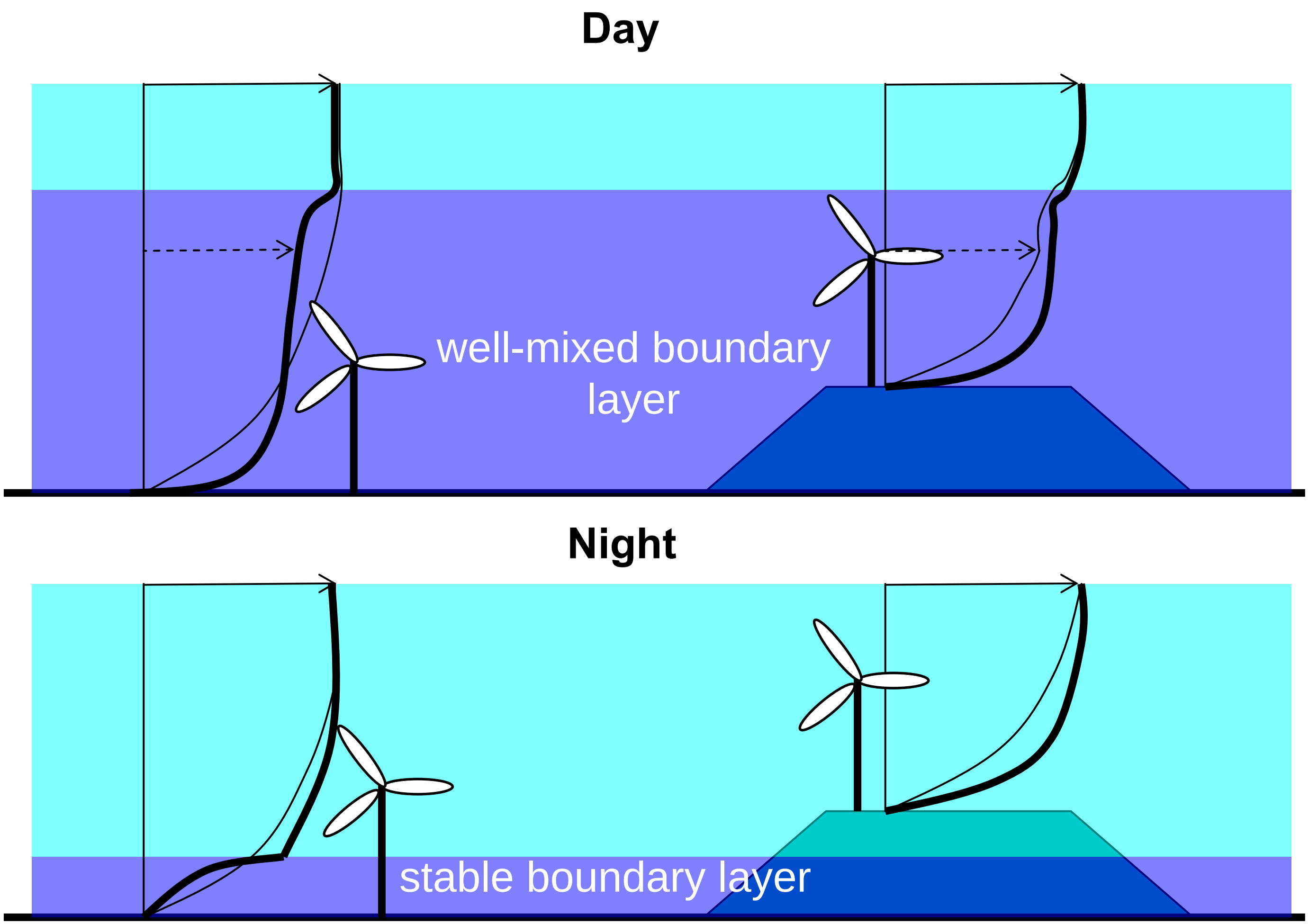

Nocturnal low-level jet and the turning of wind direction with height

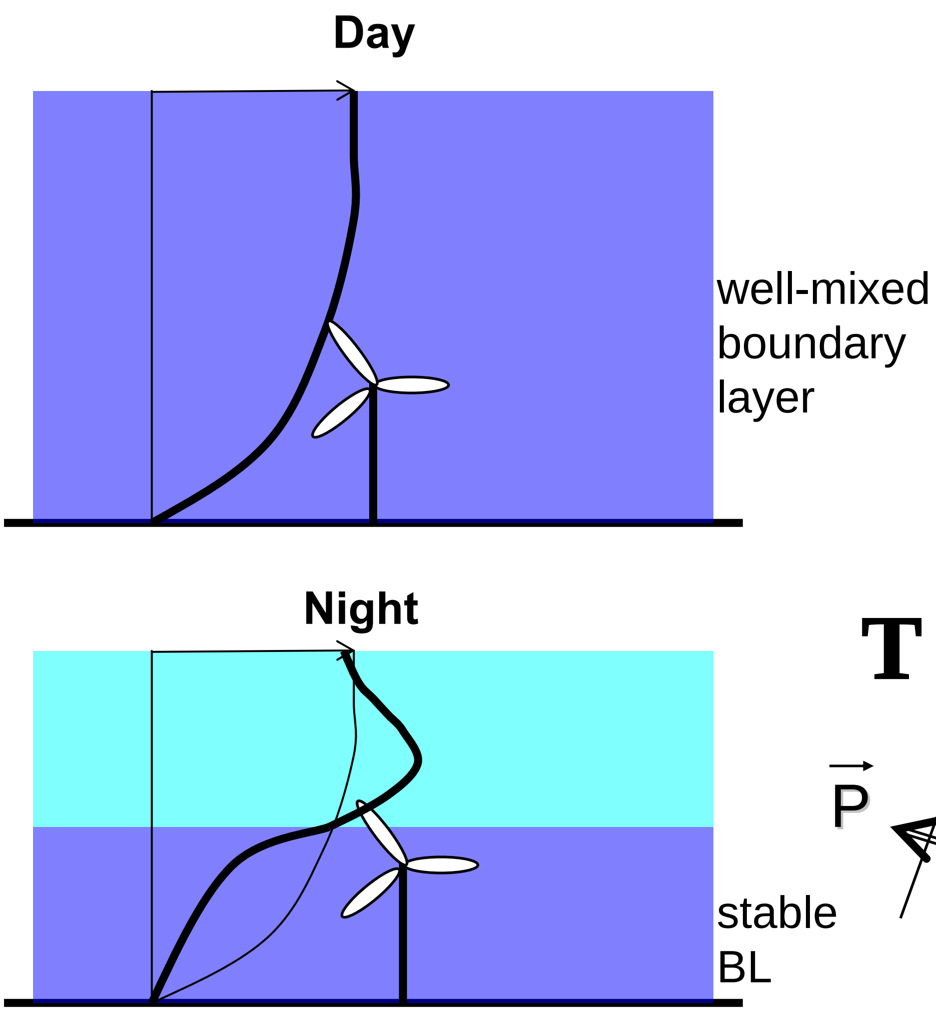

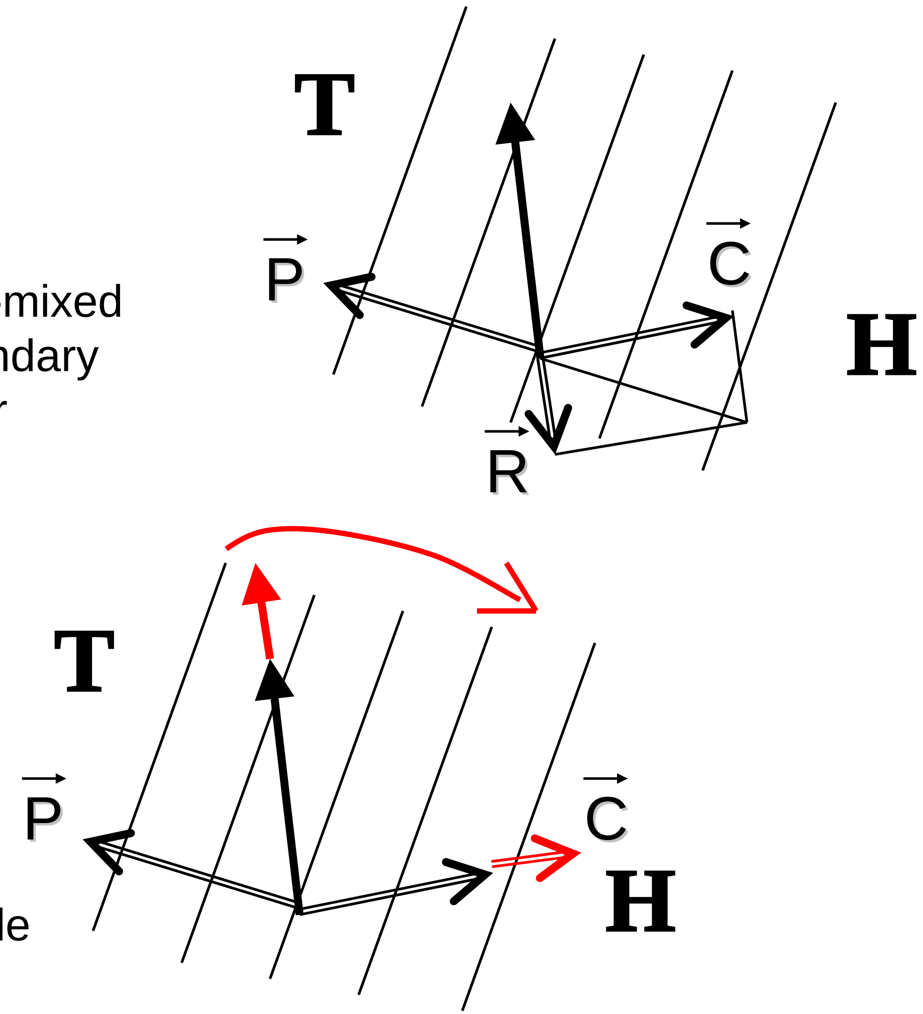

Mean diurnal variation of wind turning

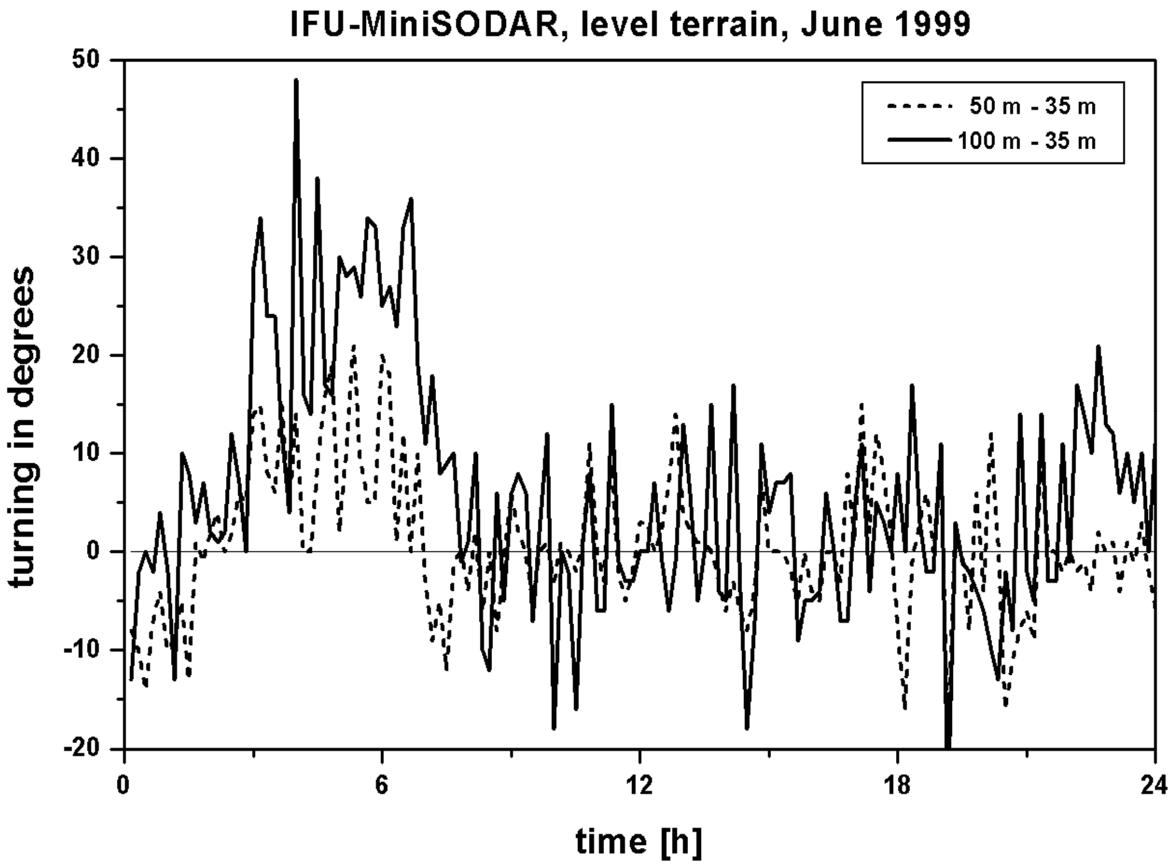

extreme example for wind turning

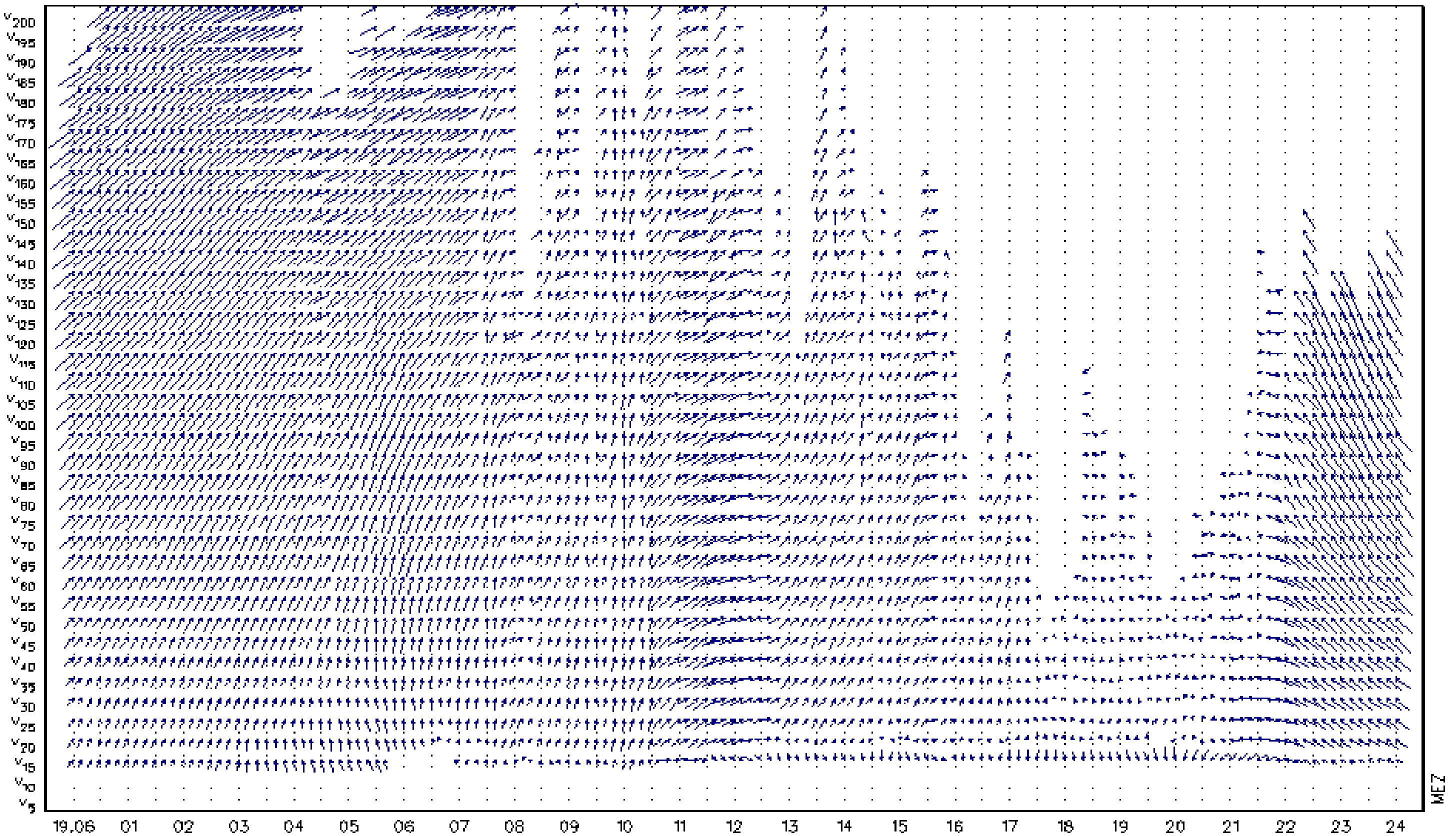

Abb.: 10'–Mittel des Windvektors (v_x) für ausgewählte Höhen (x)
IFU–MiniSODAR Sachsen–Anhalt Juni 1999

→ = 3 m/s Westwind

IFU GAP

The vertical wind profile

logarithmic law
(with stability correction) $u(z) = (u_*/\kappa)\,(\ln(z/z_0) - \psi(z/L_*))$

power law $u(z) = u(z_A)\,(z/z_A)^n$

New proposal
(Gryning et al. 2007)

$$u(z) = \frac{u_{*0}}{\kappa}\left(\ln\left(\frac{z}{z_0}\right) + \frac{z}{L_{MBL,N}} - \frac{z}{z_i}\left(\frac{z}{2L_{MBL,N}}\right)\right)$$

needs information on the PBL or mixing-layer height

Gryning et al., 2007: On the extension of the wind profile over homogeneous terrain beyond the surface boundary layer. Bound.-Lay. Meteorol., **124**, 251–268.

Mixing-layer height

Inversion height	literally: inversion in the temperature profile, increase of temperature with height, strong decrease of moisture, radiation inversions, sinking inversions, surface inversions, lifted inversions
Mixing-layer height	defined by the turbulence profile, upper boundary for vertical exchange (mixing), upper boundary of the well-mixed layer, entrainment
Boundary layer height	SBL: at night, height of the near-surface layer influenced by surface friction CBL: at day, height of convective plumes

boundary layer height ≈ mixing-layer height

boundary layer height ≥ inversion height

Basic remote sensing techniques

name	princple	spatial resolution	direction	type
RADAR	backscatter, electro-magnetic pulses, fixed wave length	profiling	scanning, slanted	active, monostatic
SODAR	backscatter, acoustic pulses, fixed wave length	profiling	fixed, slanted, vertical	active, usually monostatic
LIDAR	backscatter, optical pulses, fixed wave length(s)	profiling	scanning, fixed, horizontal, slanted, vertical	active, monostatic
RASS	backscatter, acoustic, electro-magnetic, fixed wave length	profiling	fixed, vertical	active, monostatic
	absorption, infrared, spectrum	path-averaging	fixed, horizontal, slanted	active, bistatic or passive
FTIR	emission, infrared, spectrum	path-averaging	fixed, horizontal, slanted	passive
DOAS	absorption, optical, fixed wave lengths	path-averaging	fixed, horizontal	active, bistatic
radiometry	electro-magnetic, fixed wave length(s)	averaging, profiling	fixed, scanning, slanted, vertical	passive
tomography	travel time, acoustic, fixed wave length	horizontal distribution	fixed, horizontal	active, multiple emitters and receivers

subject of this lecture

subject of this lecture

Typical frequency bands for remote sensing of the atmosphere

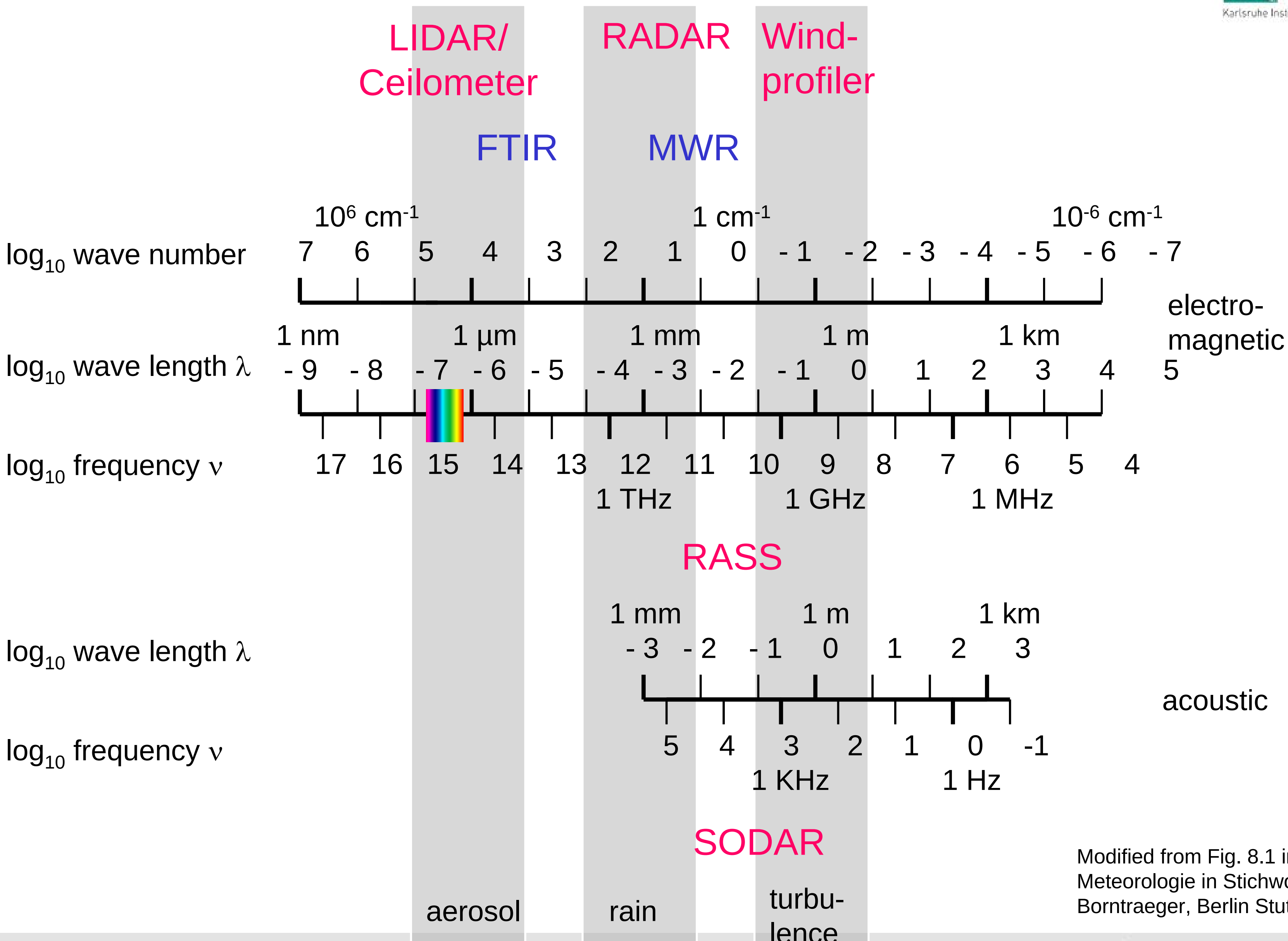

Modified from Fig. 8.1 in „ Meteorologie in Stichworten“, Borntraeger, Berlin Stuttgart 2000

SODAR

algorithms for mixing-layer height

monostatic SODAR: measuring principles

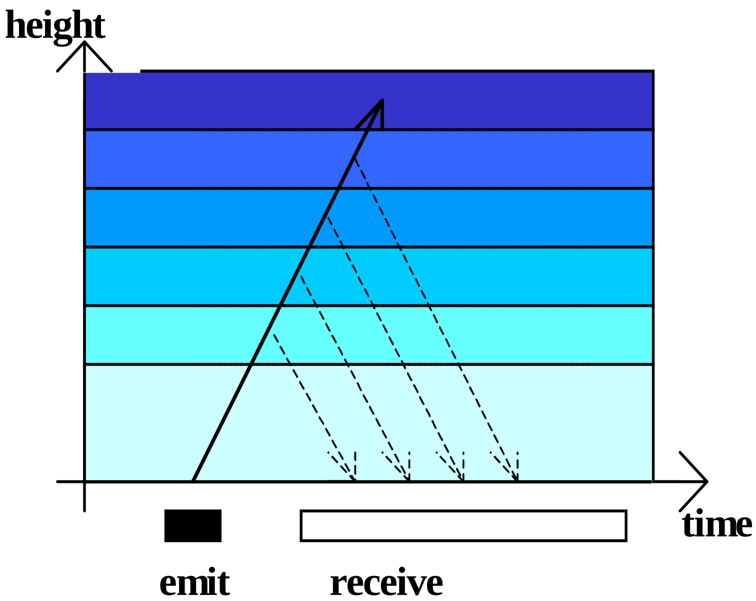

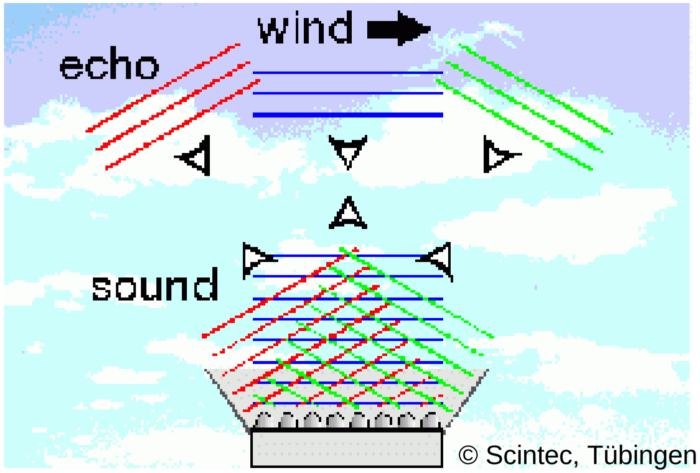

deduction:

sound travel time = height
backscatter intensity = turbulence
Doppler-shift = wind speed

Emission of sound waves into three directions:

in order to measure all three components of the wind (horizontal and vertical)

The SODAR equation:

$$P_R = r^{-2} (c_s \tau A \varepsilon / 2) P_0 \beta_s e^{-2\sigma r} + P_{bg}$$

received power P_R,
emitted power P_0,
antenna efficiency ε,
effective antenna area A,
sound absorption in air σ due to classical and molecular absorption due to the collision of water molecules with the oxygen and nitrogen molecules of the air,
distance between the scattering volume and the instrument r,
pulse duration τ (typically between 20 and 100 ms),
backscattering cross-section β_s (typically in the order of 10^{-11} m^{-1} sr^{-1}),
sound speed c_s,
background noise P_{bg}.

Emitted power: ~ 10^3 W, received (backscattered) power: 10^{-15} W

The SODAR equation:

$$P_R = r^{-2}\,(c_s \tau A \varepsilon/2)\; P_0\; \beta_s\; e^{-2\sigma r} + P_{bg}$$

The ratio of the two terms on the right-hand side of the SODAR equation is called signal-to-noise ratio (usually abbreviated as SNR).

The backscattering cross-section β_s is a function of the temperature structure function C_T^2 (Tatarskii 1961).

For a monostatic SODAR we find (Reitebuch 1999) when using the wave number $k = 2\pi/\lambda$:

$$\beta_s(180°) = 0{,}00408\; k^{1/3}\; C_T^2\; /T^2$$

Reitebuch, O., 1999: SODAR-Signalverarbeitung von Einzelpulsen zur Bestimmung hochaufgelöster Windprofile. Schriftenreihe des Fraunhofer-Instituts für Atmosphärische Umweltforschung, Shaker Verlag GmbH Aachen, Bd. 62, 178 S.

Tatarskii, V.I., 1971: The effect of the turbulent atmosphere on wave propagation. Kefer Press, Jerusalem, 472 S.

Sample plot SODAR (convective BL at daytime)

acoustic backscatter intensity

40 – 300 m

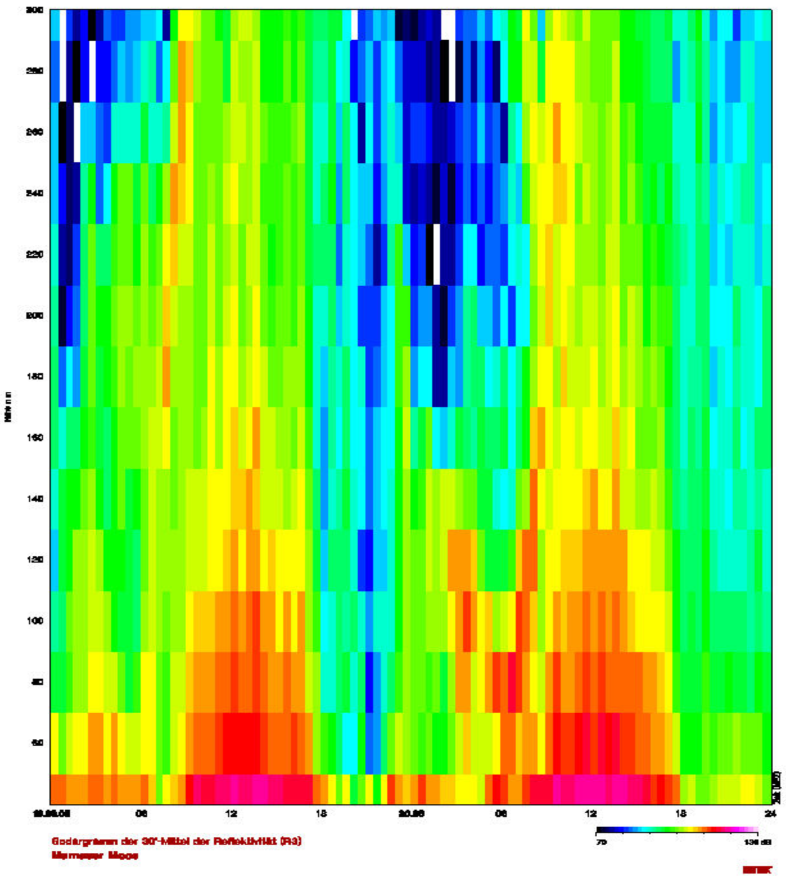

2 days, midnight to midnight

sigma w

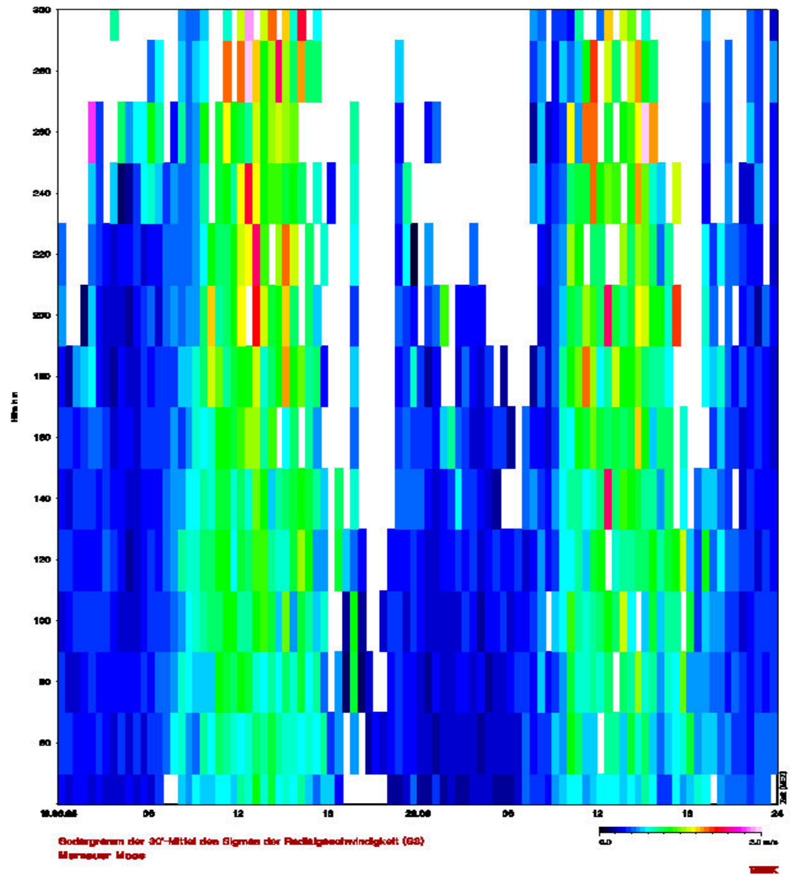

Sample plot SODAR (lifted inversion)

40 – 400 m

acoustic backscatter intensity

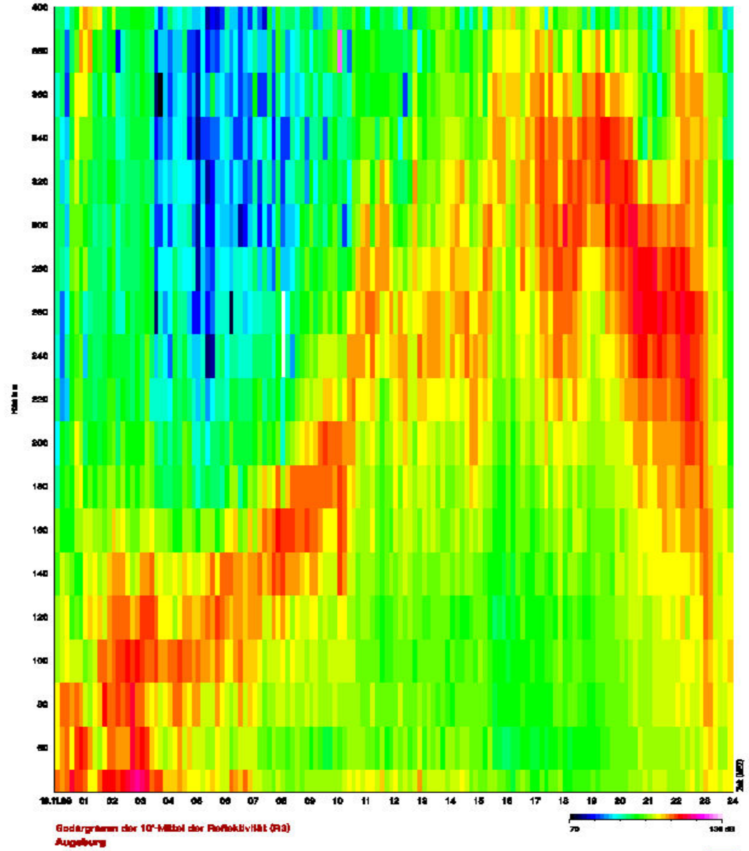

sigma w

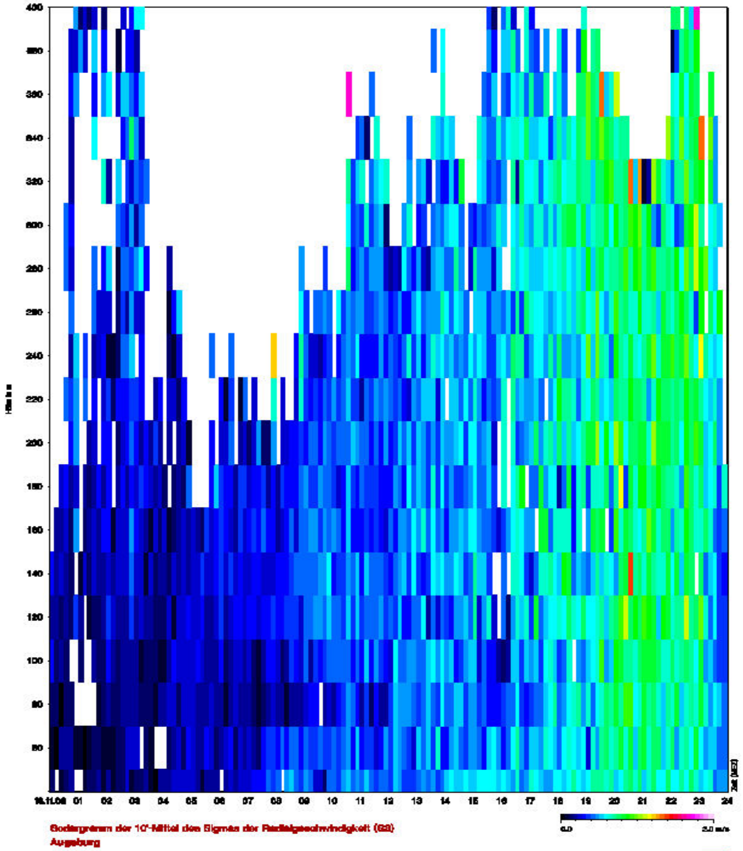

1 day, midnight to midnight

Algorithms to detect MLH from SODAR data

criterion 1:
upper edge of high turbulence

criterion 2:
surface and lifted inversions

MLH = Min (C1, C2)

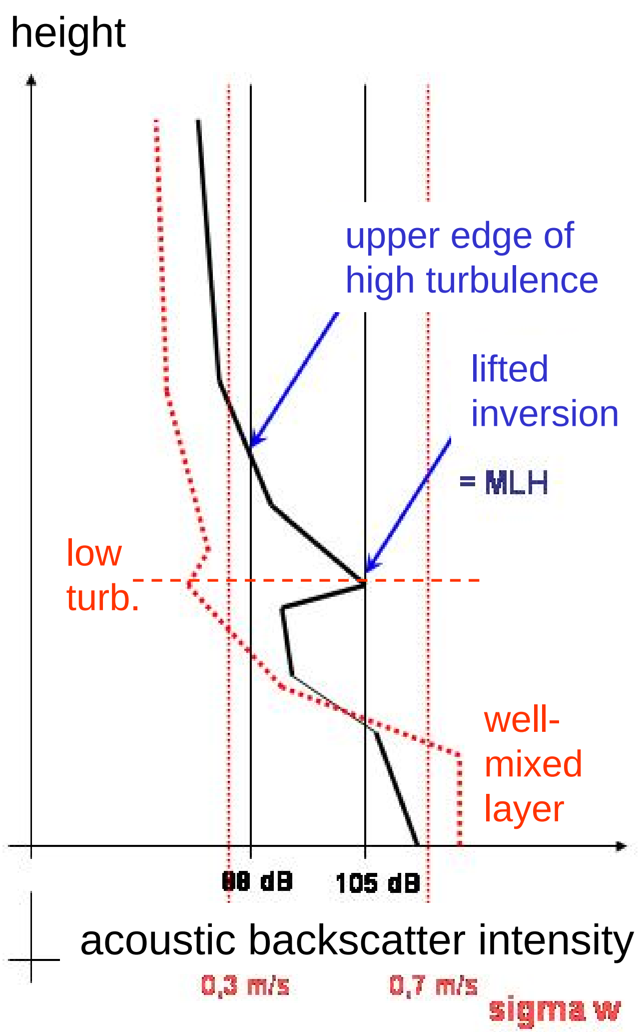

example 1: daytime

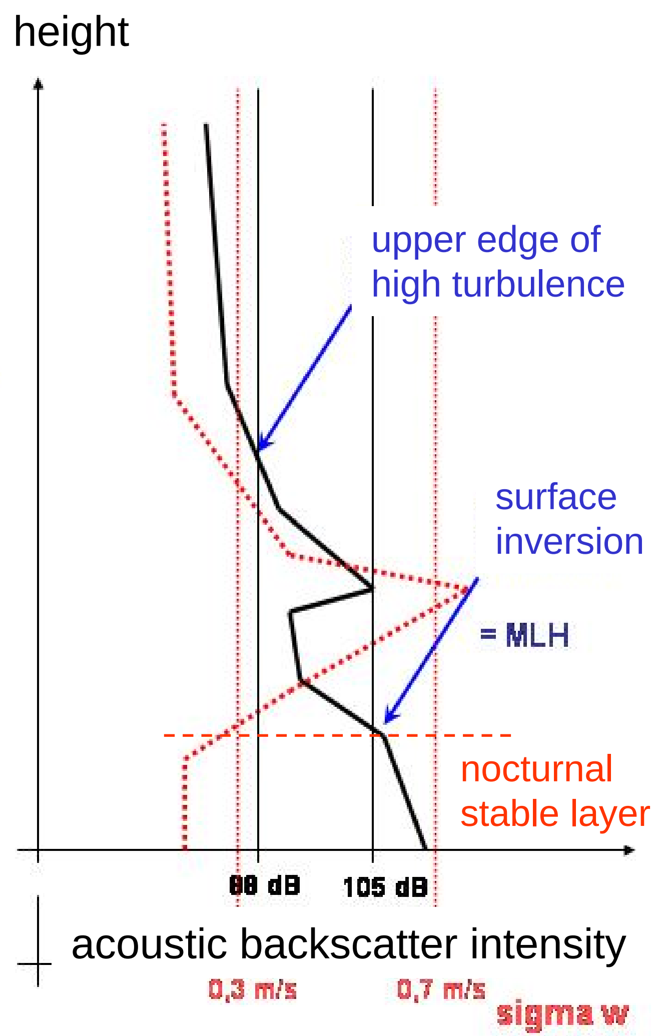

example 2: night-time

Ceilometer

algorithms for mixing-layer height

Ceilometer/LIDAR measuring principle

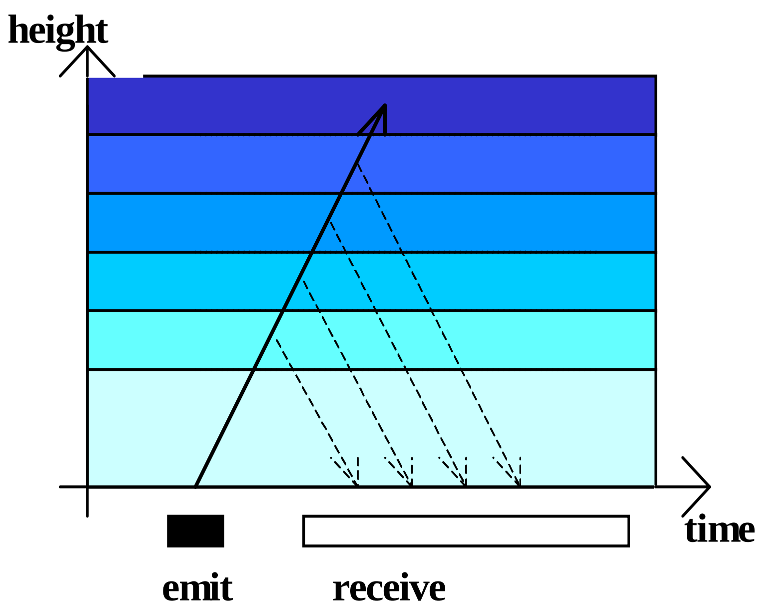

detection:

travel time of signal = height
backscatter intensity = particle size and number distribution
Doppler-shift = cannot be analyzed from ceilometer data
(only from Wind-LIDAR: velocity component in line of sight)

The LIDAR equation:

$$P_R(\lambda,r) = r^{-2}\,(c\tau A\varepsilon/2)\,P_0\,[\beta_m(\lambda,r) + \beta_p(\lambda,r)]\,e^{-2\sigma r} + P_{bg}$$

distance r between the LIDAR and the backscattering object,
speed of light c,
pulse duration τ,
antenna area A,
correction term for the detector efficiency and losses due to the lenses ε,
emitted energy P_0,
backscatter coefficient for molecules β_m and for particles β_p,
absorption of light in the atmosphere σ,
background noise P_{bg}.

For a ceilometer β_m is negligible and only β_p is important

Sample plot ceilometer (convective BL at daytime)

optical backscatter intensity

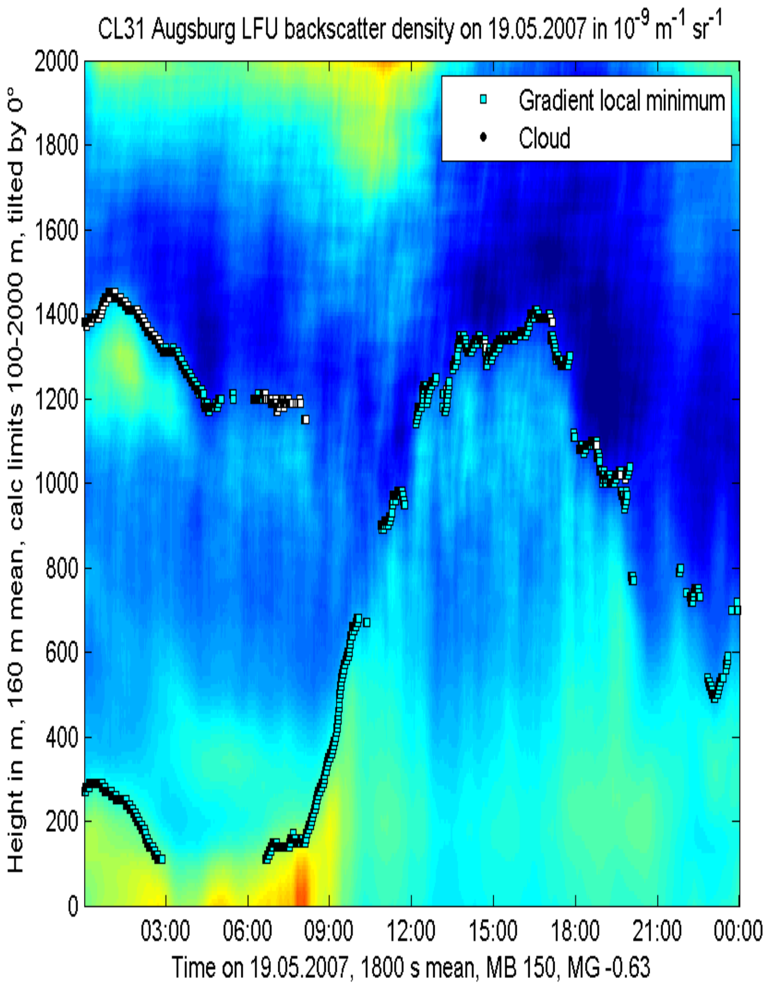

negative vertical gradient of optical backscatter intensity

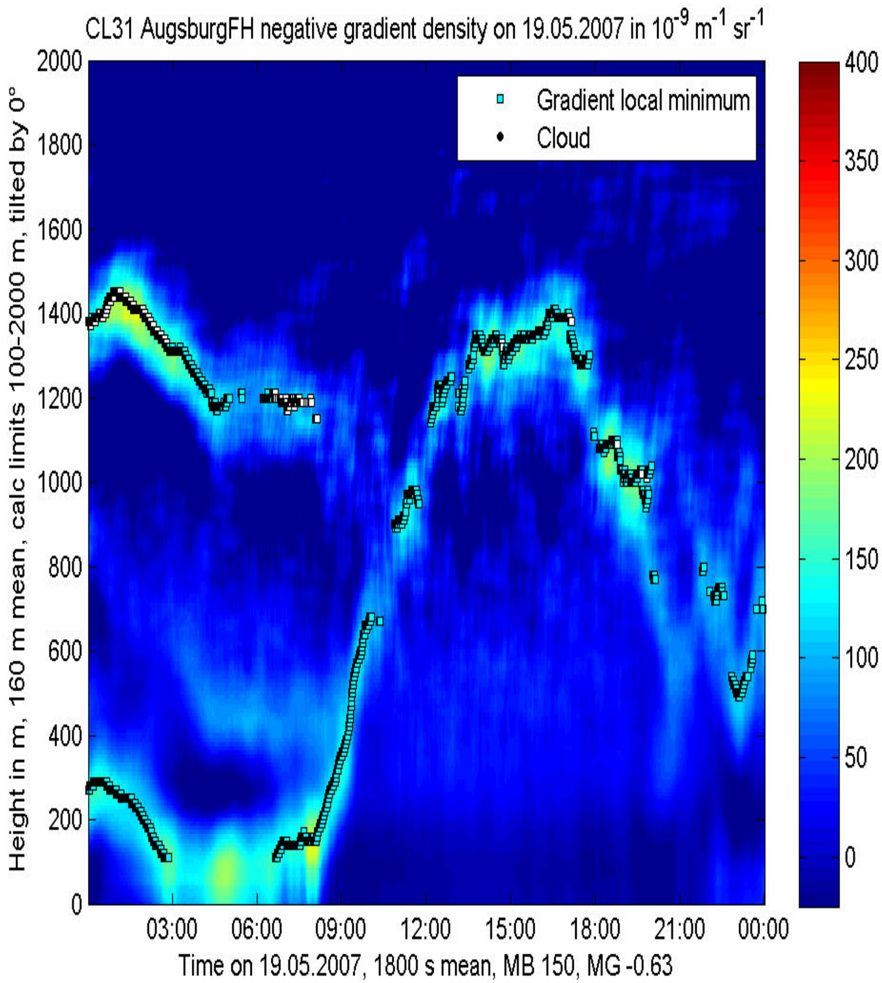

Algorithms to
detect MLH
from Ceilometer-Daten

criterion

minimal vertical gradient
of backscatter
intensity (the most
negative gradient)

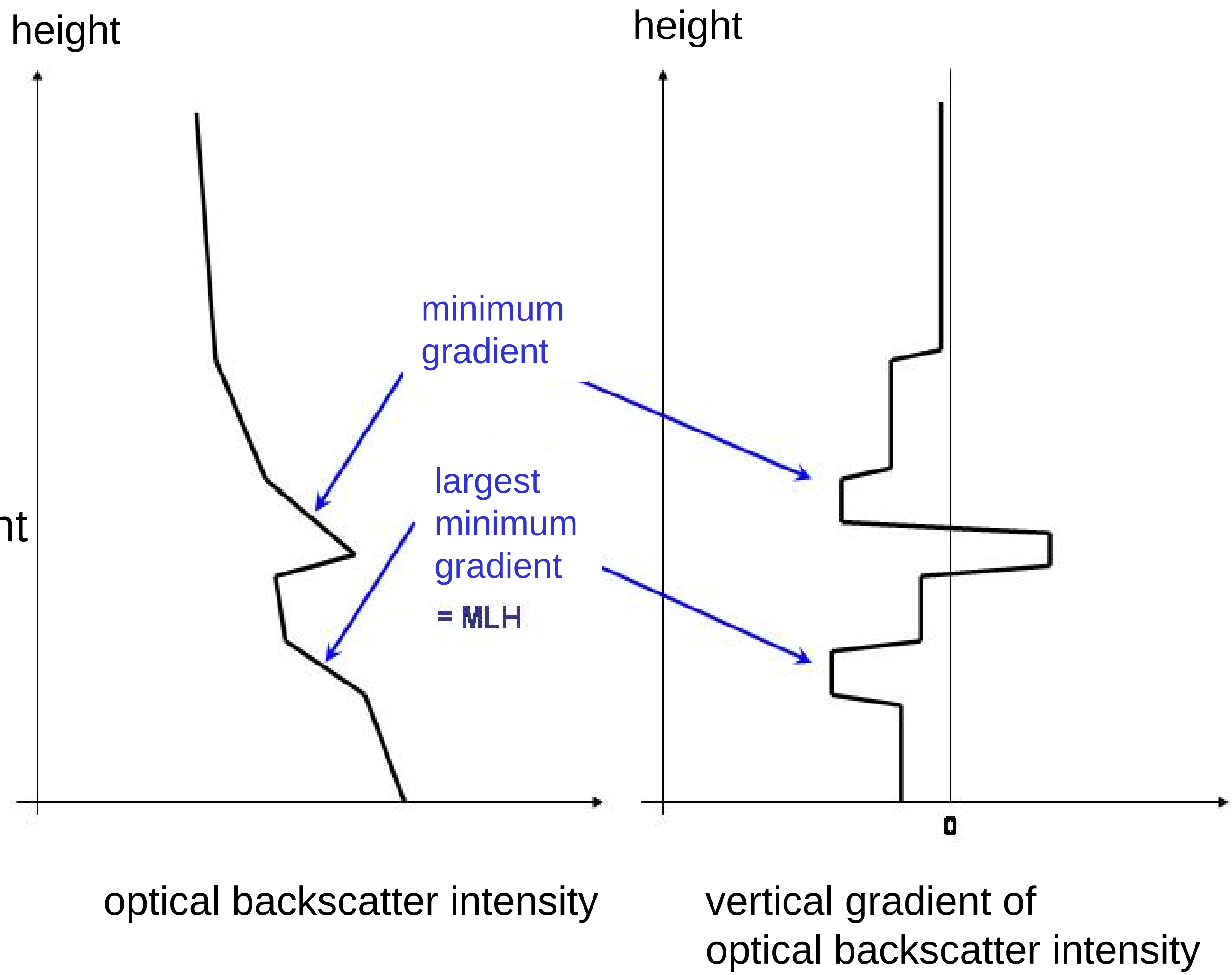

Different gradient methods (see Sicard et al. 2006, BLM 119, 135-157)

logarithmic gradient minimum

gradient minimum

inflection point method (minimum of 2nd derivative)

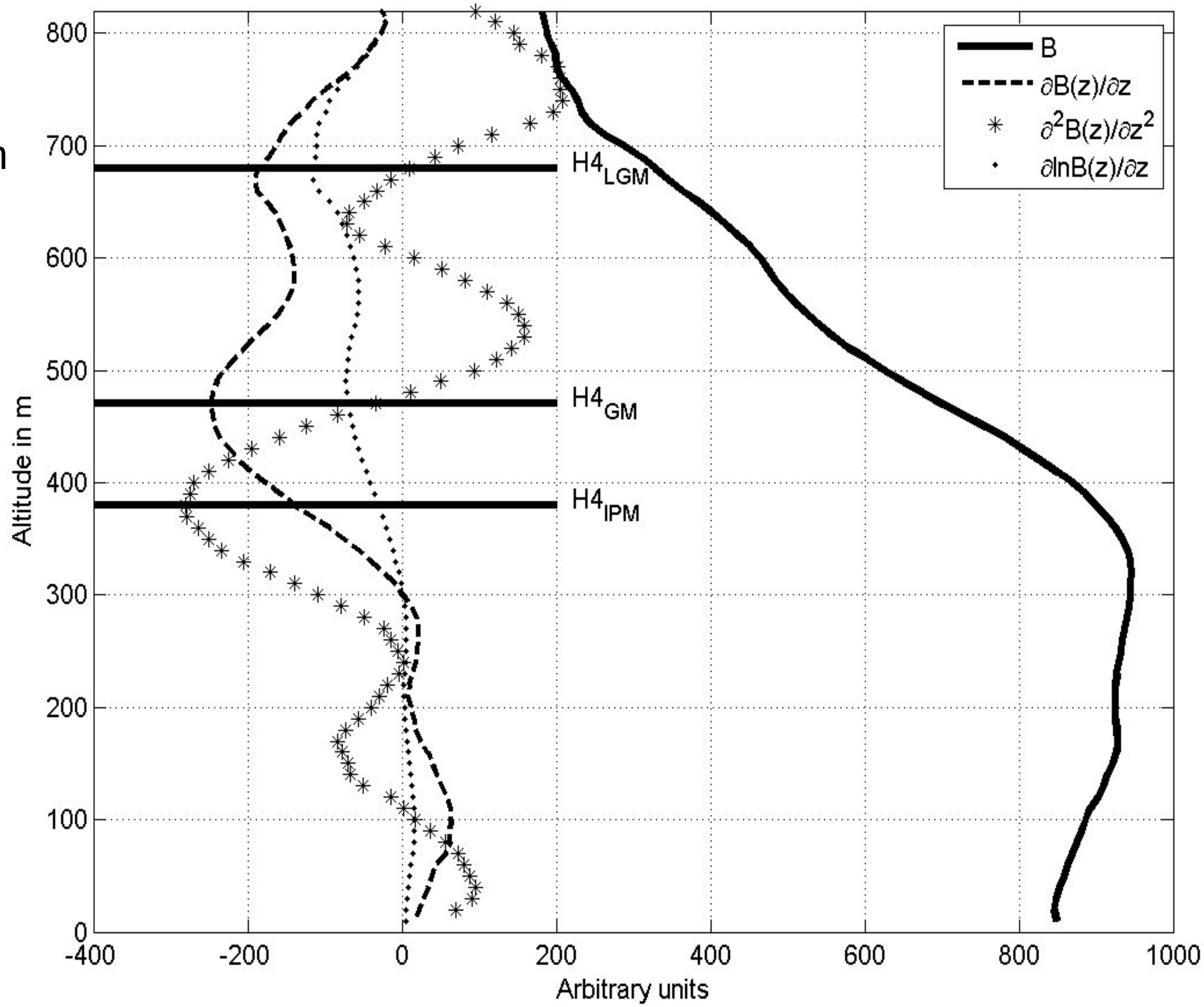

comparison of two different ceilometers

LD40

two optical axes

wave length: 855 nm
height resolution: 7.5 m
max. range: 13000 m

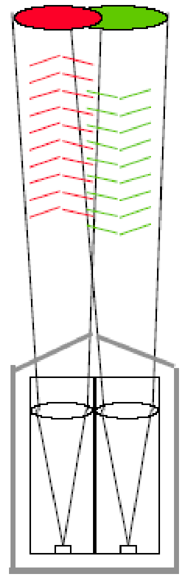

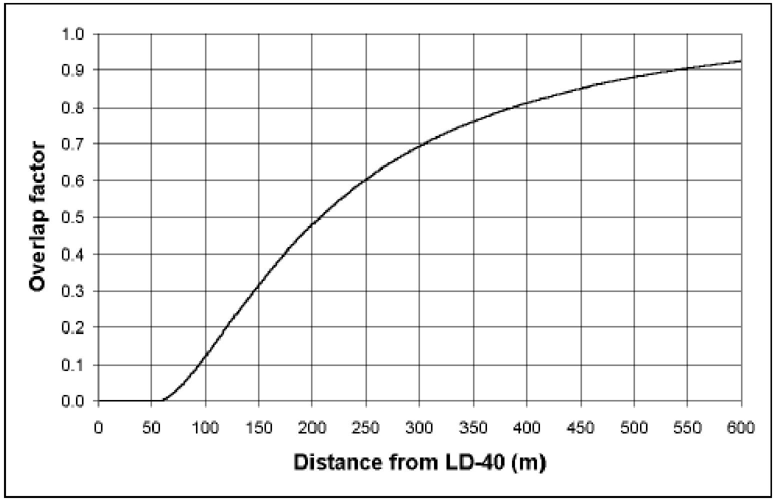

CL31

one optical axis

wave length: 905 nm
height resolution: 5 m
max. range: 7500 m

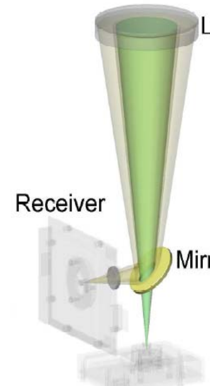

19 May 2007: ceilometer LD40 and CL31

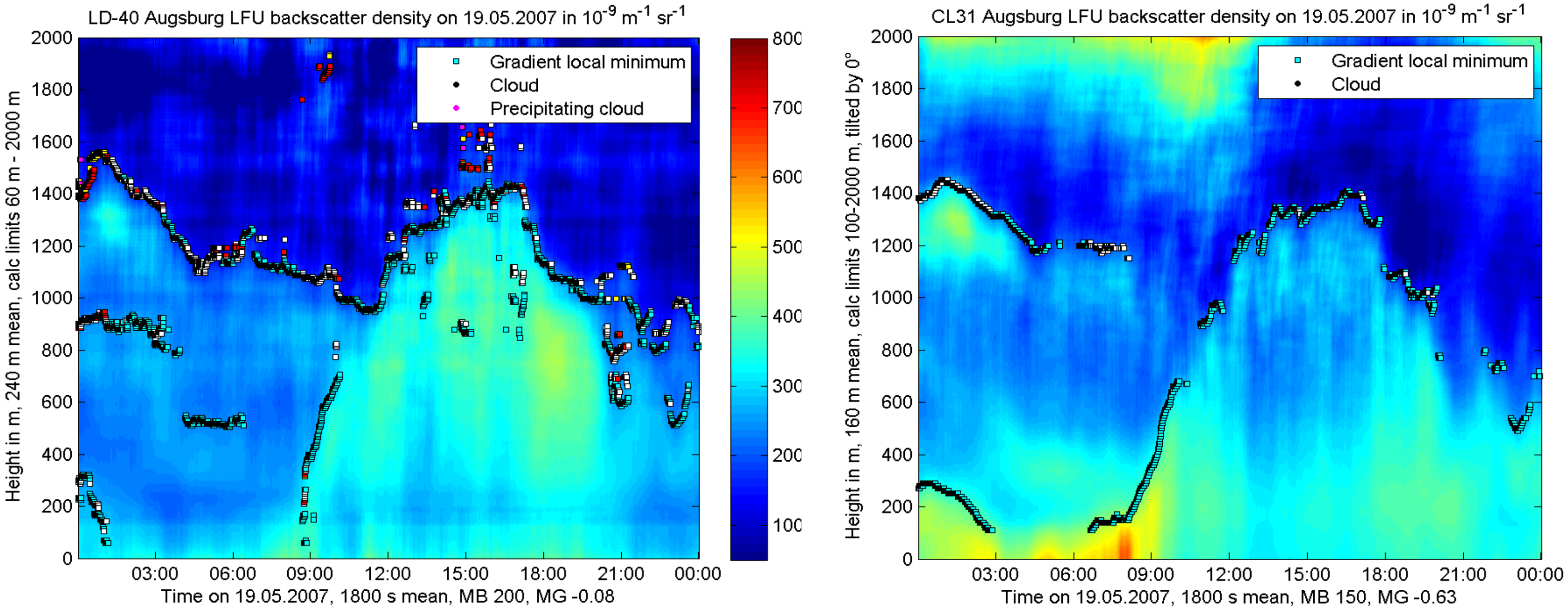

comparison of MLH from LD40 and CL31 data

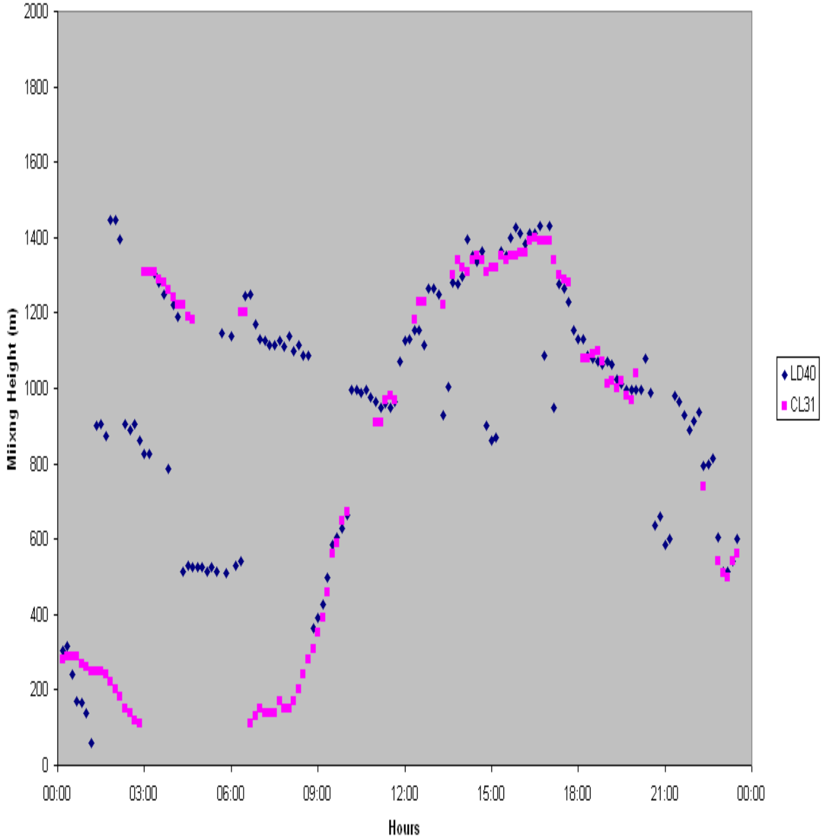

19 May 2007

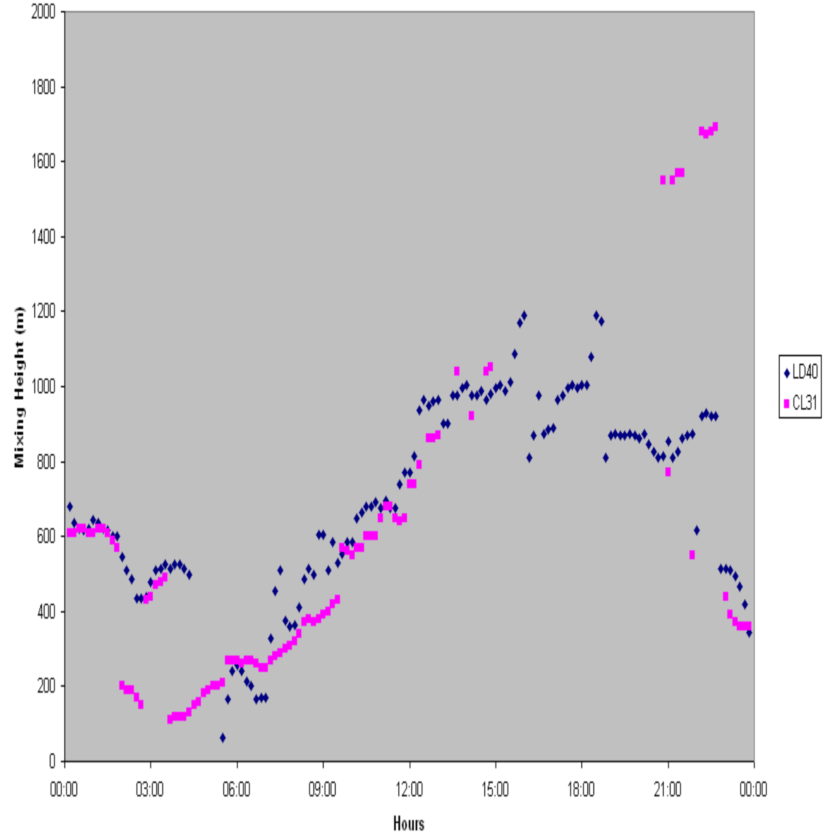

20 May 2007

Comparison SODAR and Ceilometer

Measurement of the vertical structure of the boundary layer and mixing-layer height by remote sensing:

mobile surface-based acoustic and optical remote sensing yields information on:

➔ thermal structure of the BL and turbulence intensity

(SODAR)

➔ aerosol content of the BL

(Ceilometer)

comparison of algorithms

left: SODAR

middle and right: ceilometer

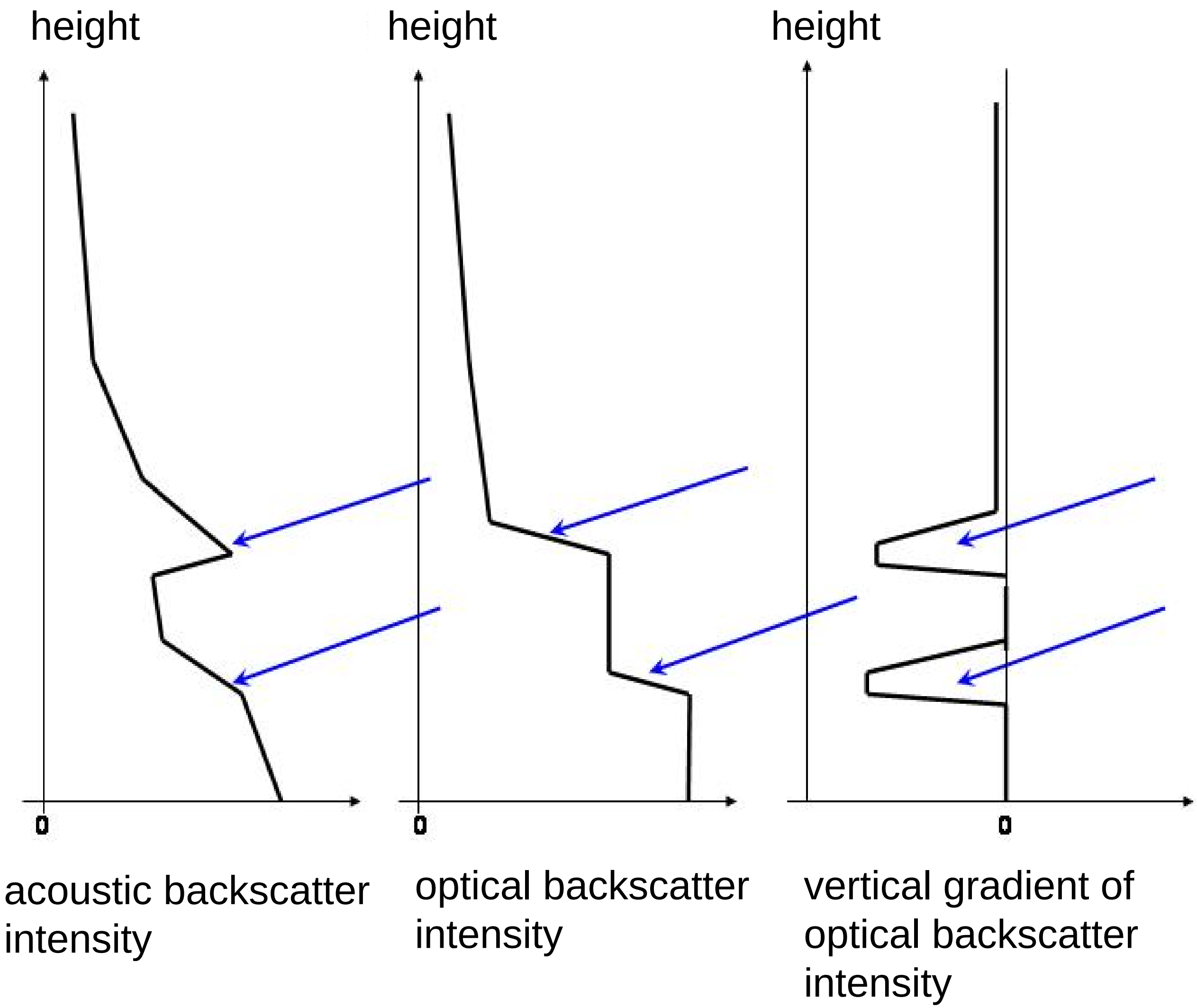

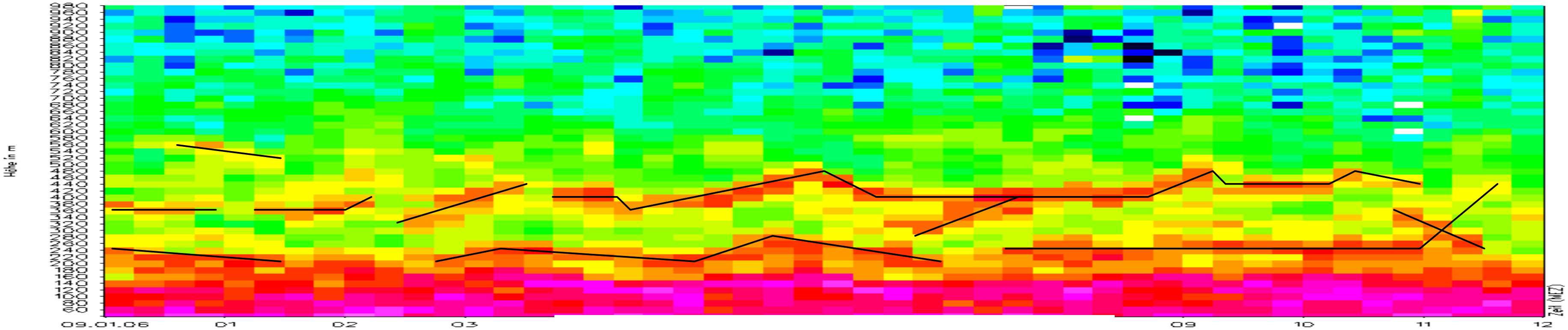

acoustic backscatter intensity

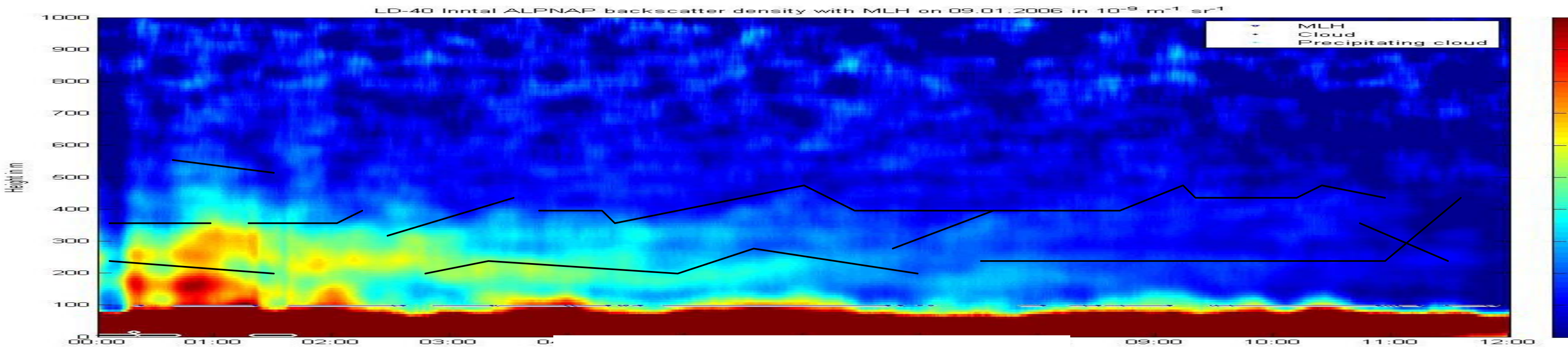

optical backscatter intensity

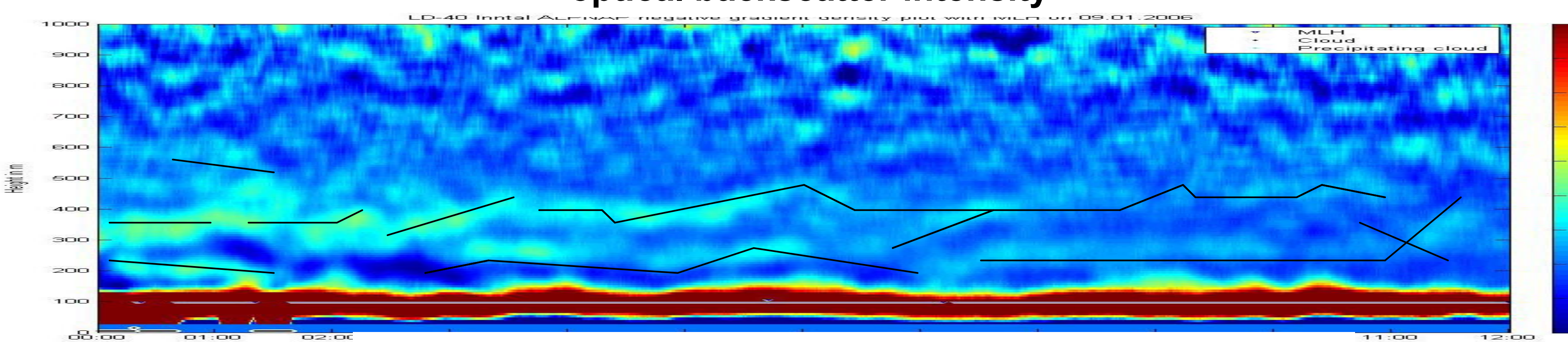

negative vertical gradient of optical backscatter intensity

Application examples for SODAR and Ceilometer

Example for the joint operation of a SODAR and a Ceilometer

winter in an Alpine valley (snow-covered)

(ALPNAP-Campaign in the Inn valley in winter 2005/06)

(ALPNAP was a project in the European Programme INTERREG III B Alpine Space, ref. no. D/III/2.1/7)

SODAR measurements in a wintry Alpine valley

29 January 2006

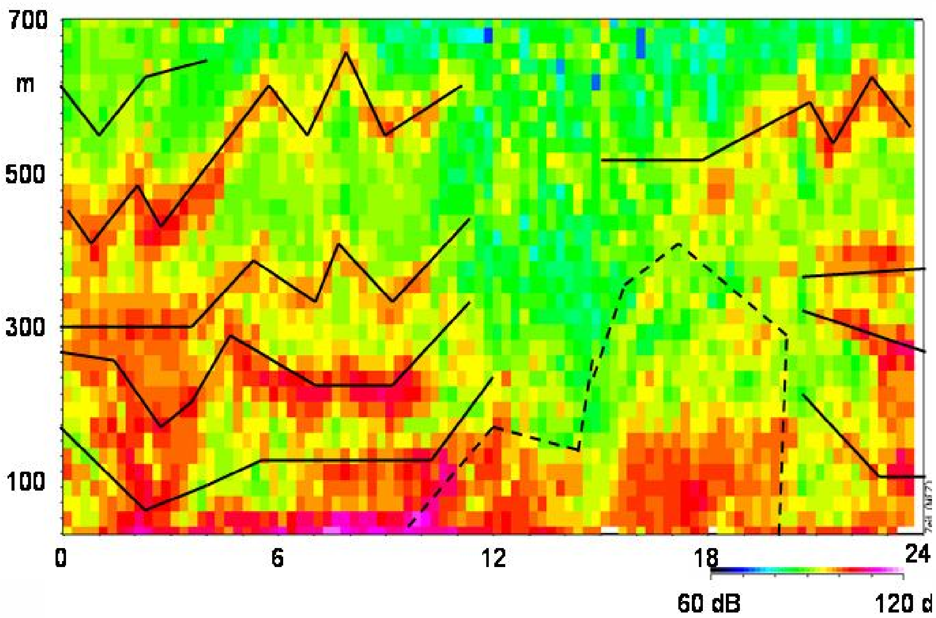

backscatter intensity

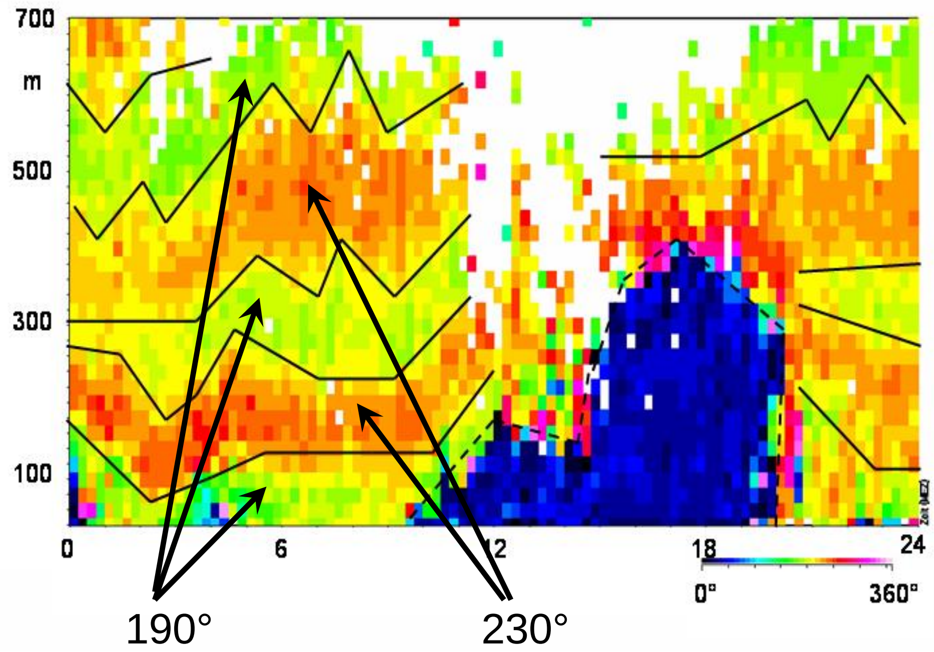

wind direction

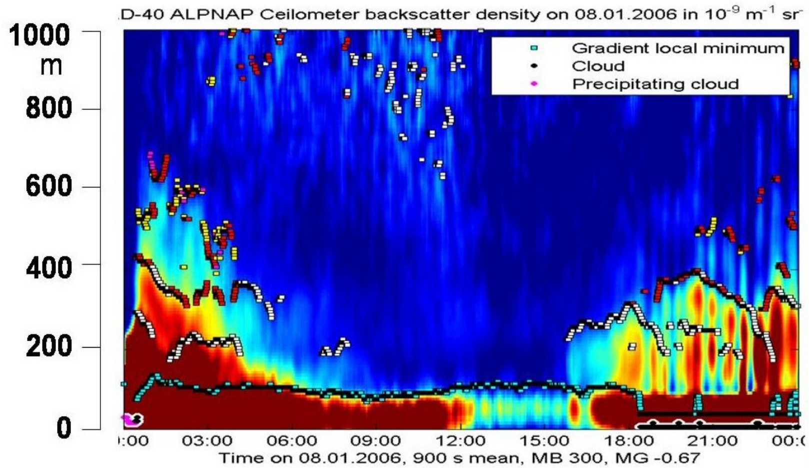

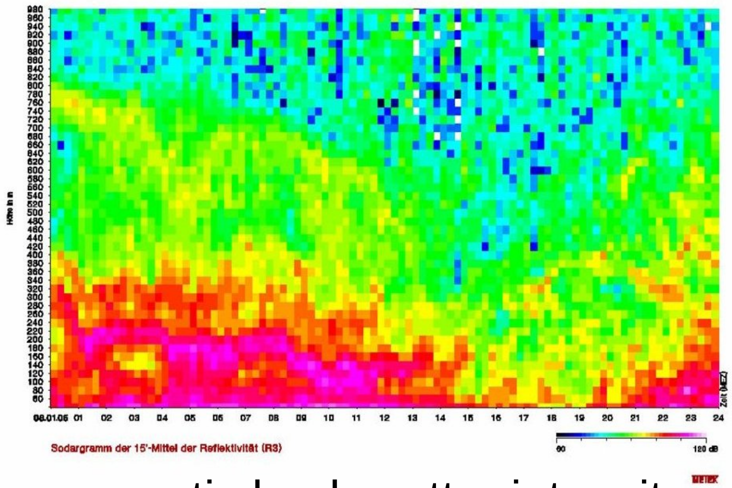

optical backscatter intensity

acoustic backscatter intensity

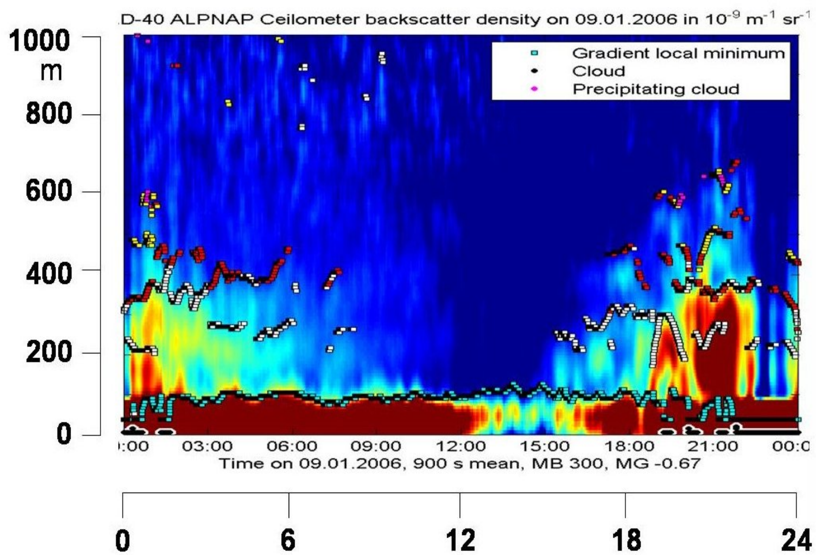

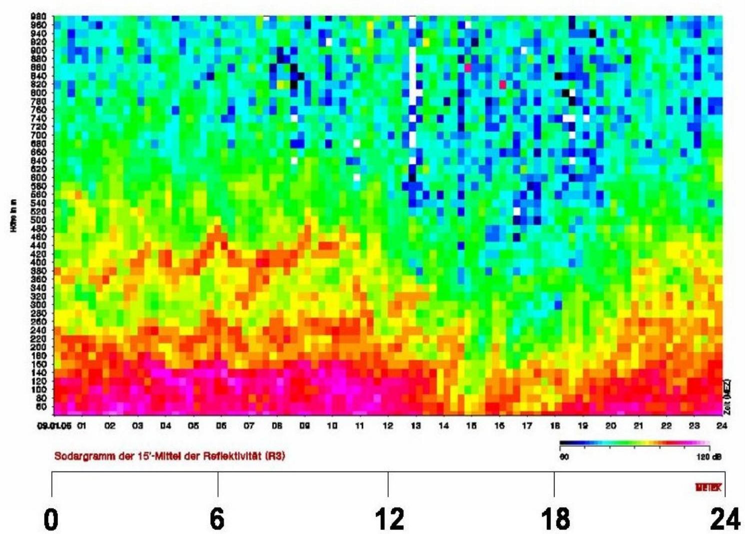

statistical evaluations of the Inn valley measurements (1-18 Jan 06)

MLH: mean diurnal variation

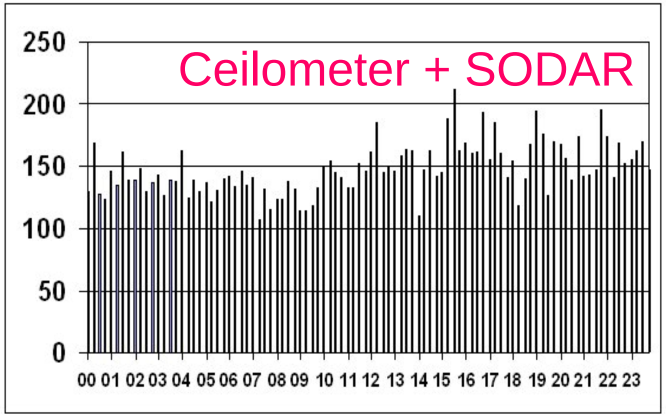

MLH: frequency distribution

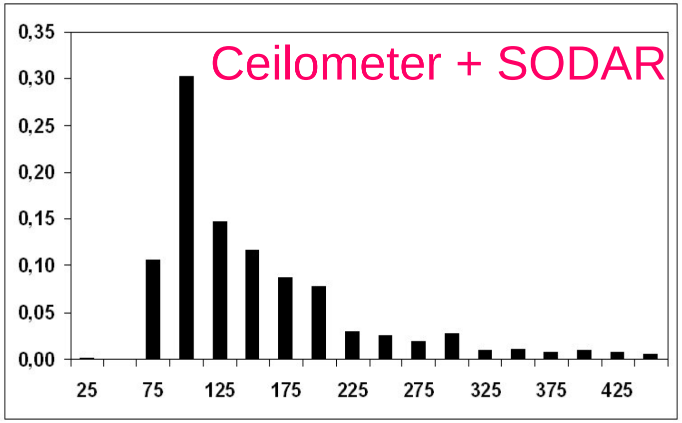

multiple inversions

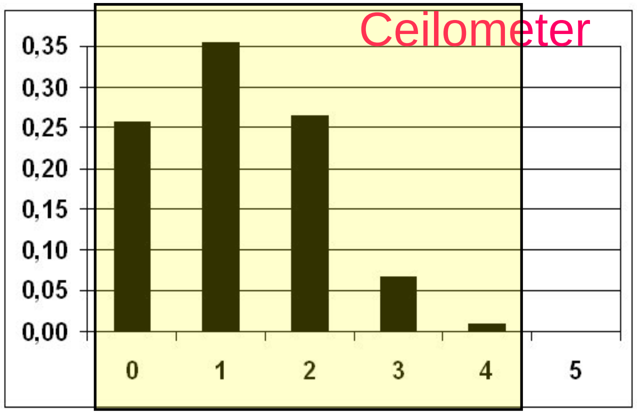

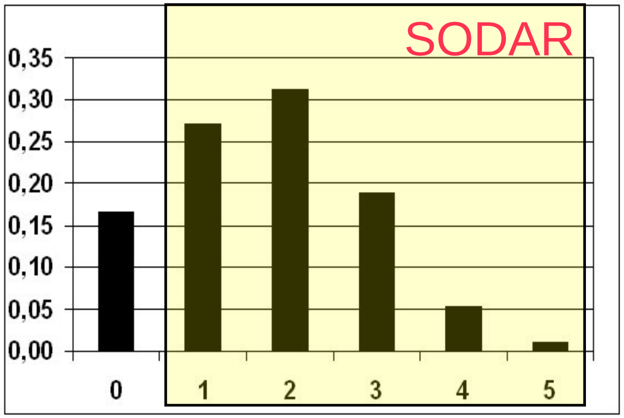

Example for the joint operation of a SODAR and a Ceilometer

summer 2003 Budapest (Hungary)

(ICAROS NET-Campaigns)

(ICAROS NET was a project within the European Research Framework Programme FP5: IST-2000-29264)

Diurnal variation of mixing-layer height from SODAR and Ceilometer data (Budapest)

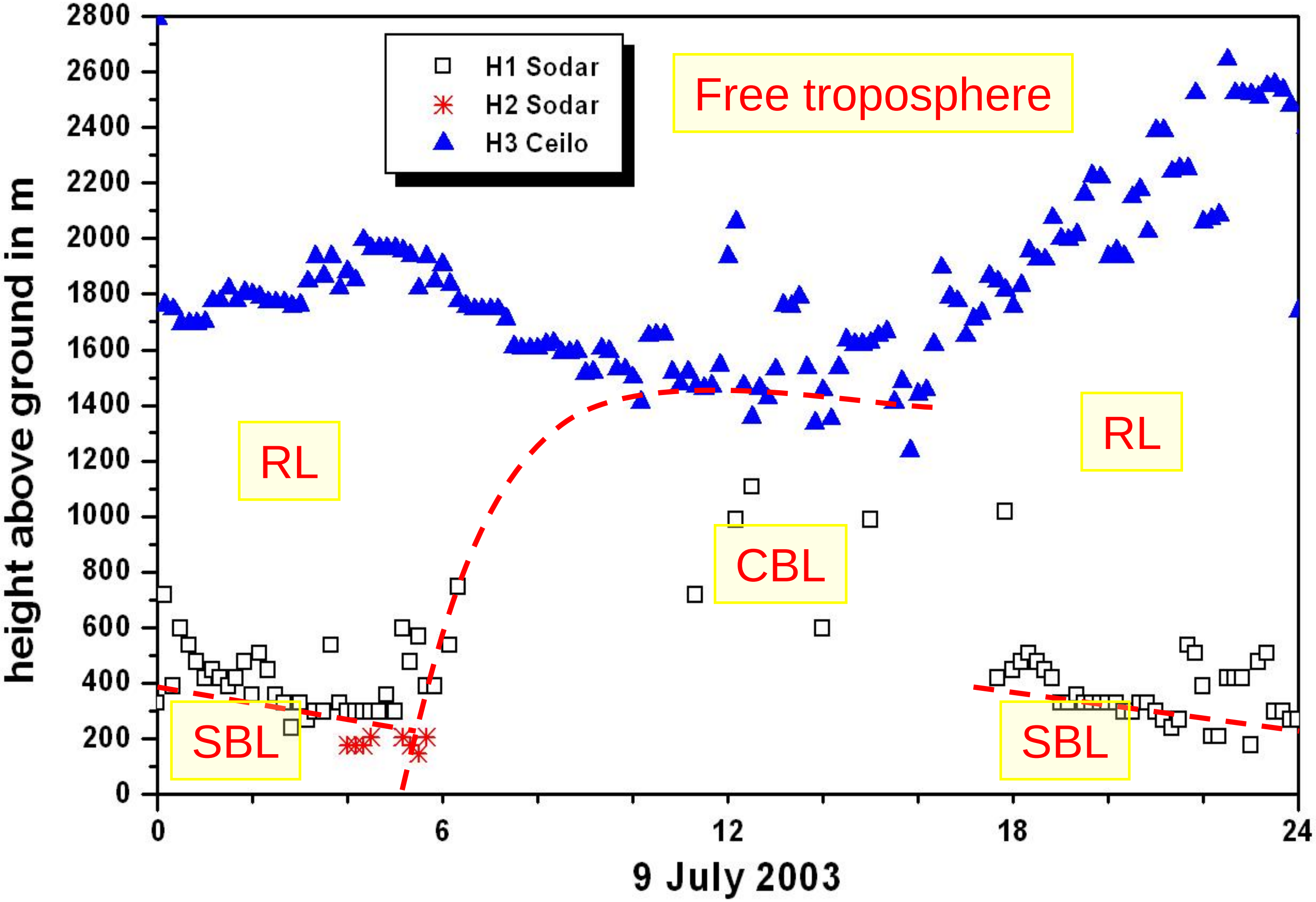

SBL:

stable boundary layer (usually at night and in winter)

CBL:

convective boundary layer (usually at daytime due to strong insolation)

RL:

residual layer (usually at night-time)

Simultaneous operation SODAR-Ceilometer: examples for summer days

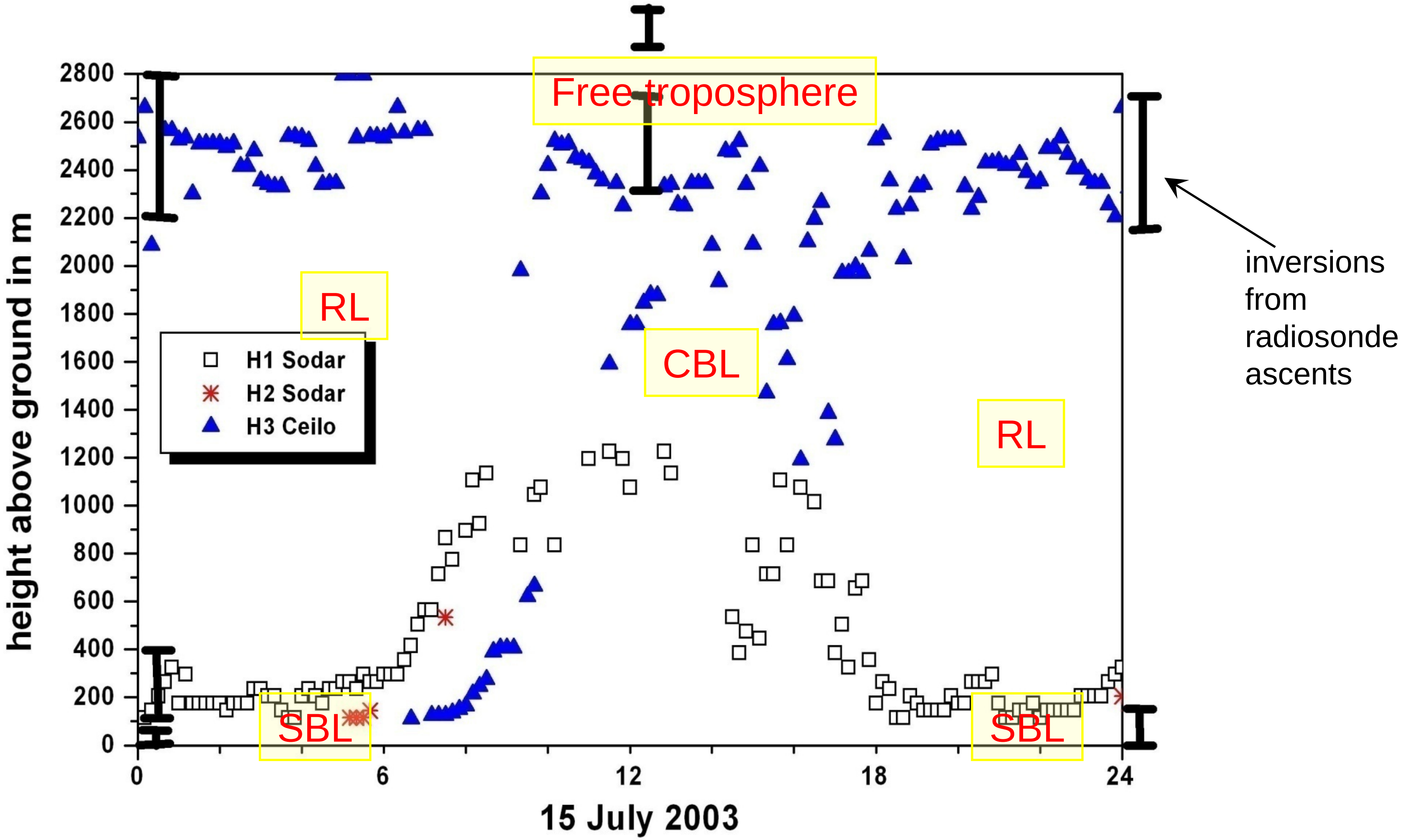

Emeis, S., K. Schäfer, 2006: Remote sensing methods to investigate boundary-layer structures relevant to air pollution in cities. Bound.-Lay Meteorol., 121, 377-385,

Example for the joint operation of a SODAR
and two ceilometers (LD40 and CL31 of Vaisala)

spatial variation of MLH over Augsburg (town with 250 000 inhabitants in Germany)

(measurement campaign in Augsburg since winter 2006/07)

(cooperation with University of Augsburg, Helmholtz Centre Munich (health impact research), State Environmental Agency of Bavaria, City of Augsburg)

comparison of optical (top) and acoustic (below) backscatter intensity

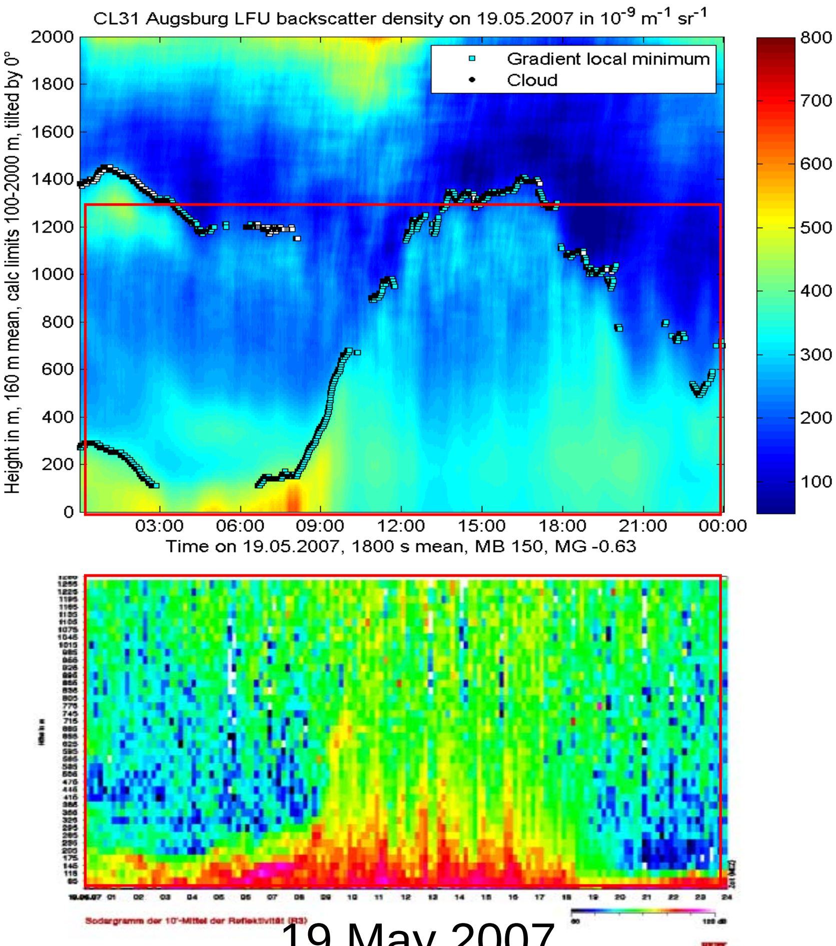

19 May 2007

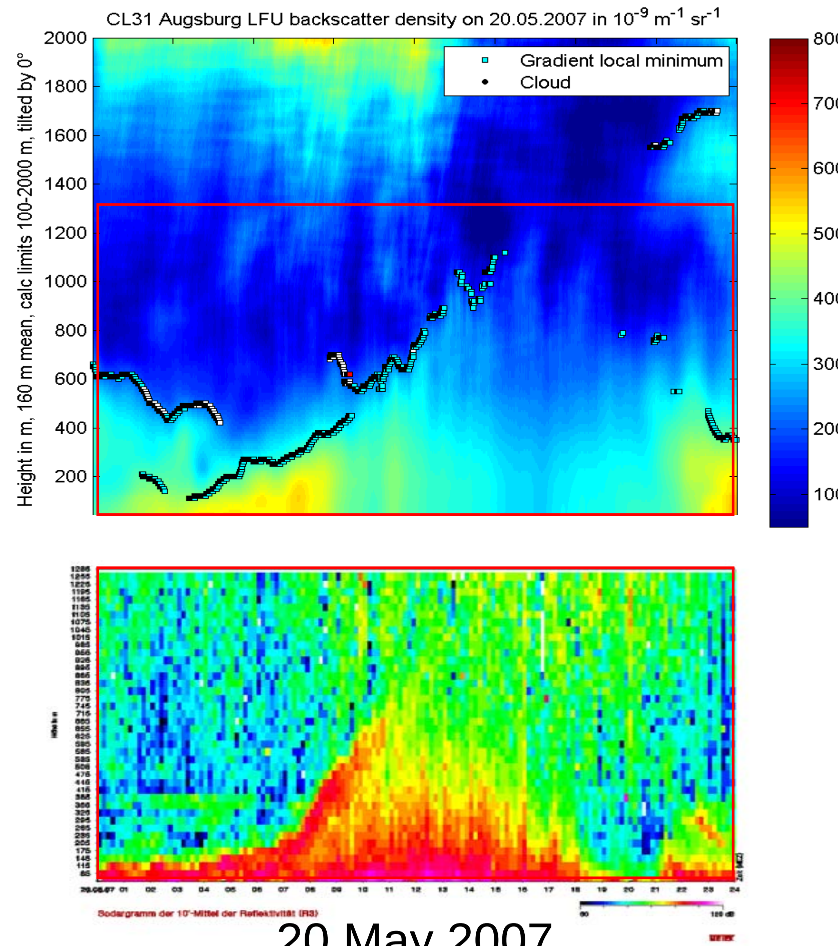

20 May 2007

comparison of MLH from Sodar and CL31 data

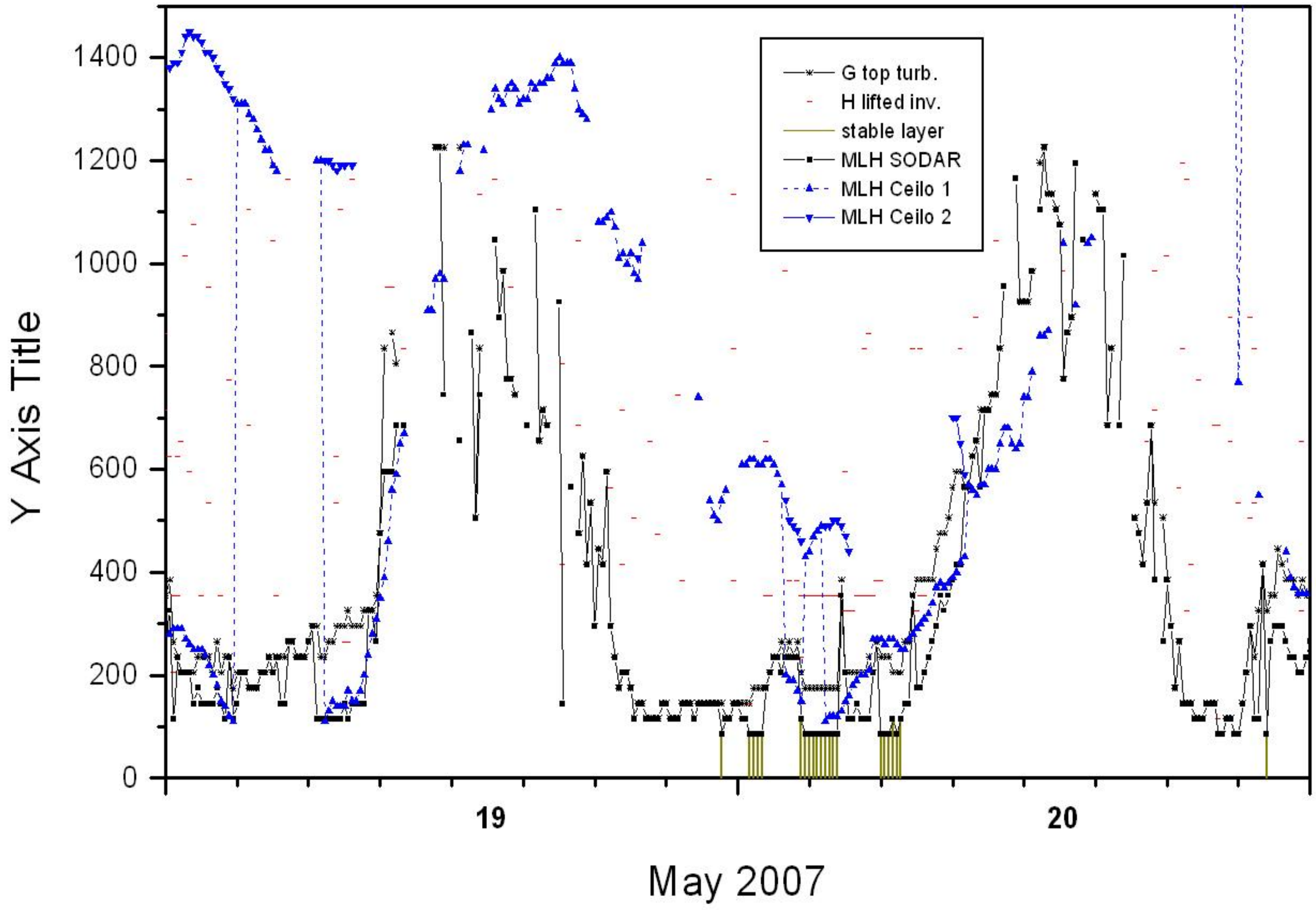

RASS

principles of operation

examples

RASS (radio-acoustic remote sensing)

measures vertical temperature profiles

Bragg-RASS: windprofiler plus acoustic component

Doppler-RASS: SODAR plus electro-magnetic component

UHF RASS (boundary layer)

VHF RASS (troposphere)

RASS: frequencies

Bragg condition: acoustic wavelength = ½ electro-magnetic wavelength

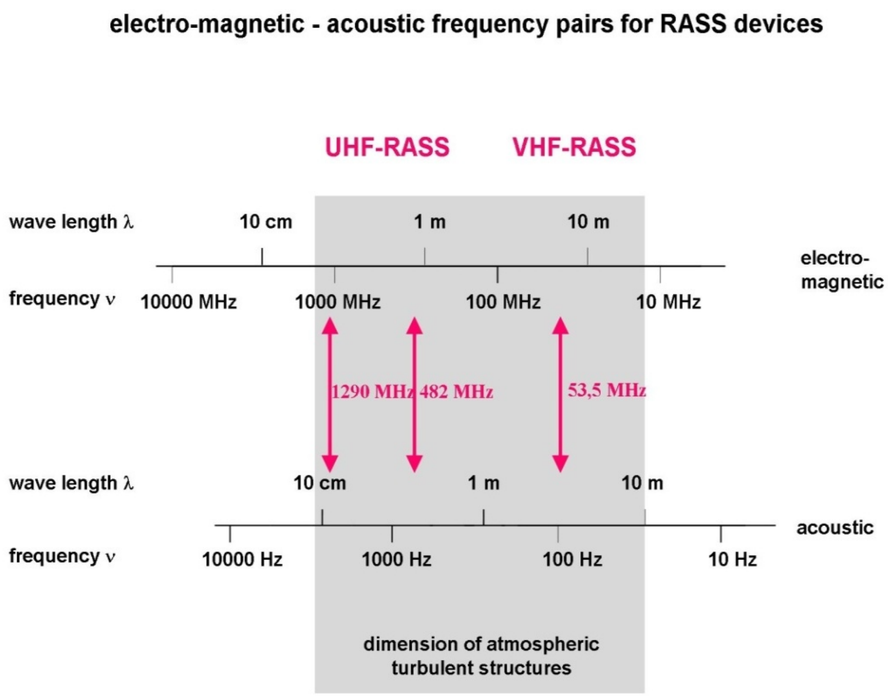

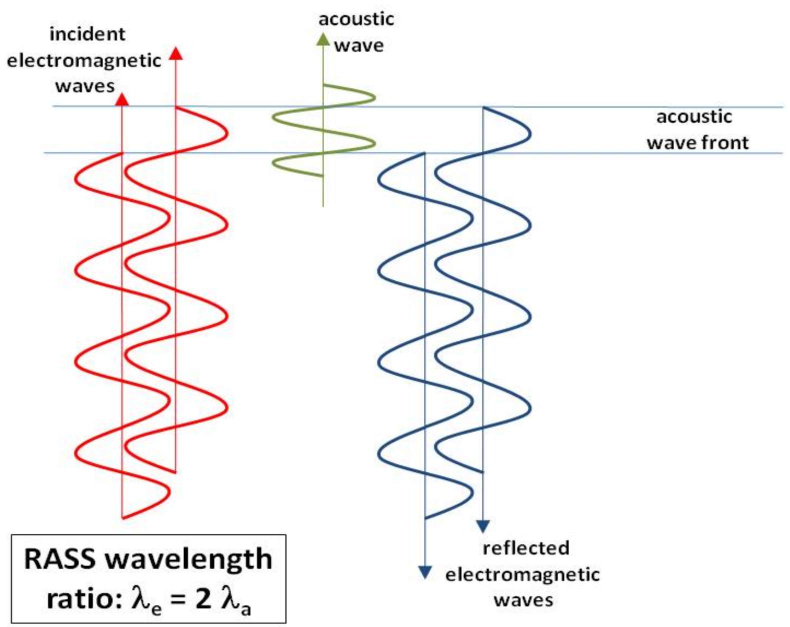

SODAR-RASS
(Doppler-RASS)

(METEK)

acoustic frequ.: 1500 – 2200 Hz
radio frequ.: 474 MHz
resolution: 20 m
lowest
range gate: ca. 40 m

vertical range: 540 m

Bragg-RASS

acoustic frequ.: about 3000 Hz
radio frequ.: 1290 MHz
resolution: 50 m
lowest
range gate: ca. 200 m

vertical range: 1000 m

example RASS data: summer day
potential temperature (left), horizontal wind (right)

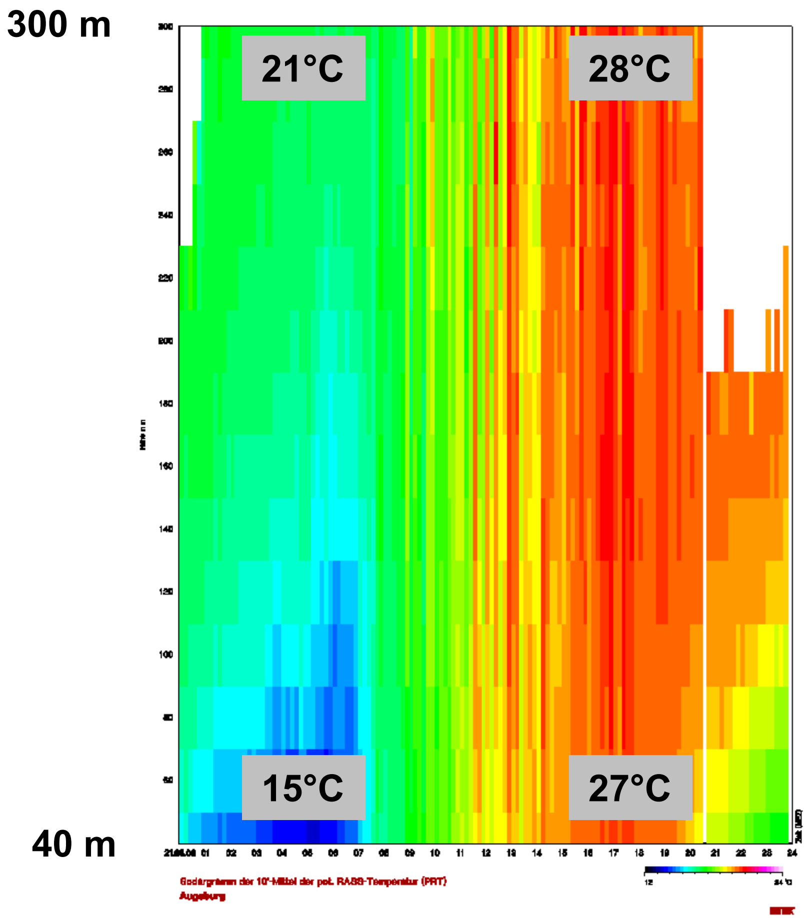

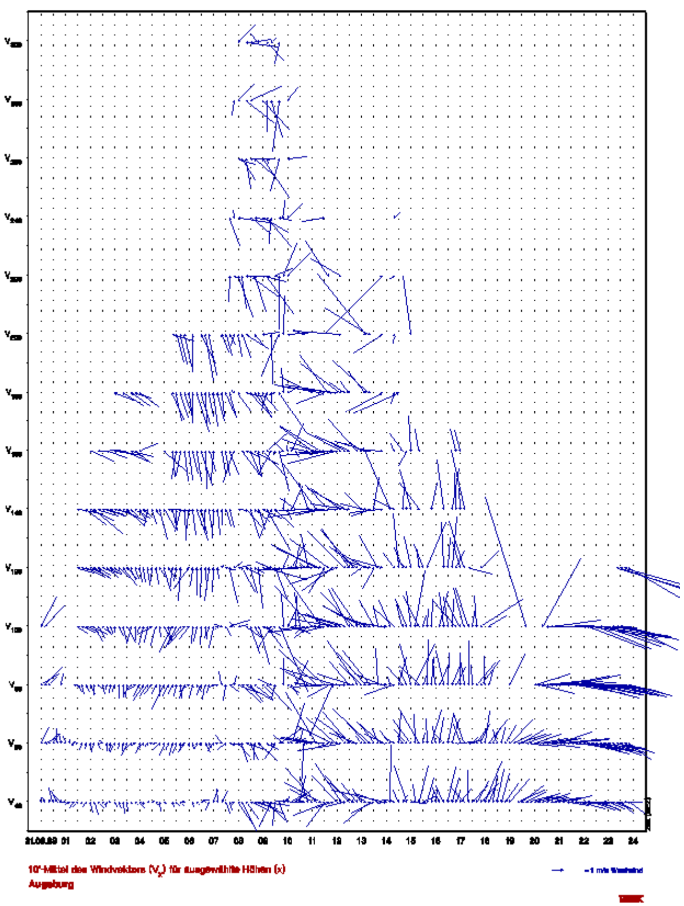

example RASS data: winter day
potential temperature (left), horizontal wind (right)

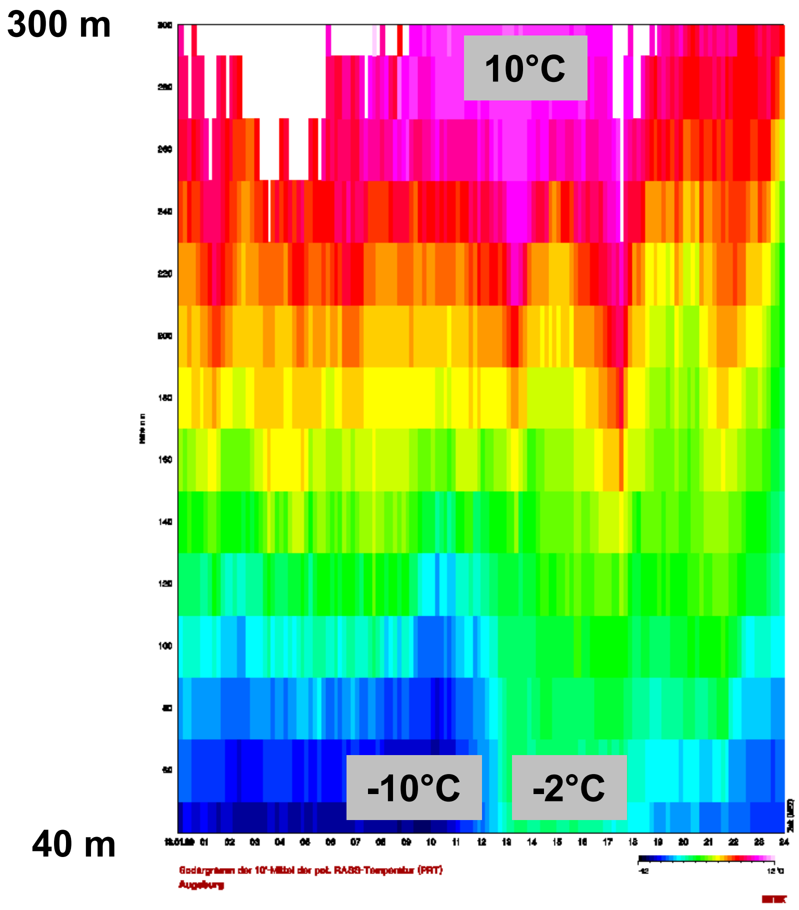

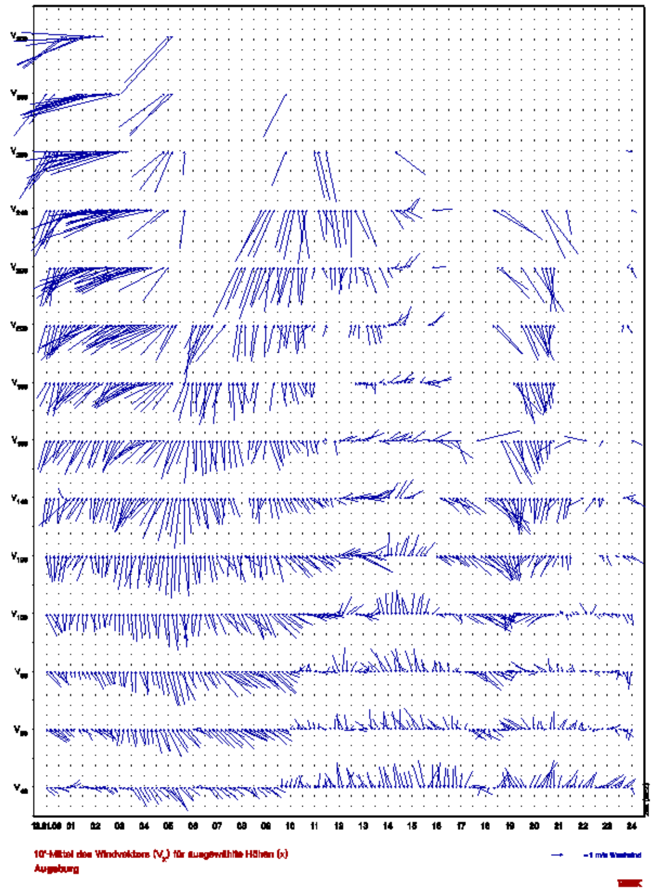

example RASS data: inversion
potential temperature (left), horizontal wind (right)

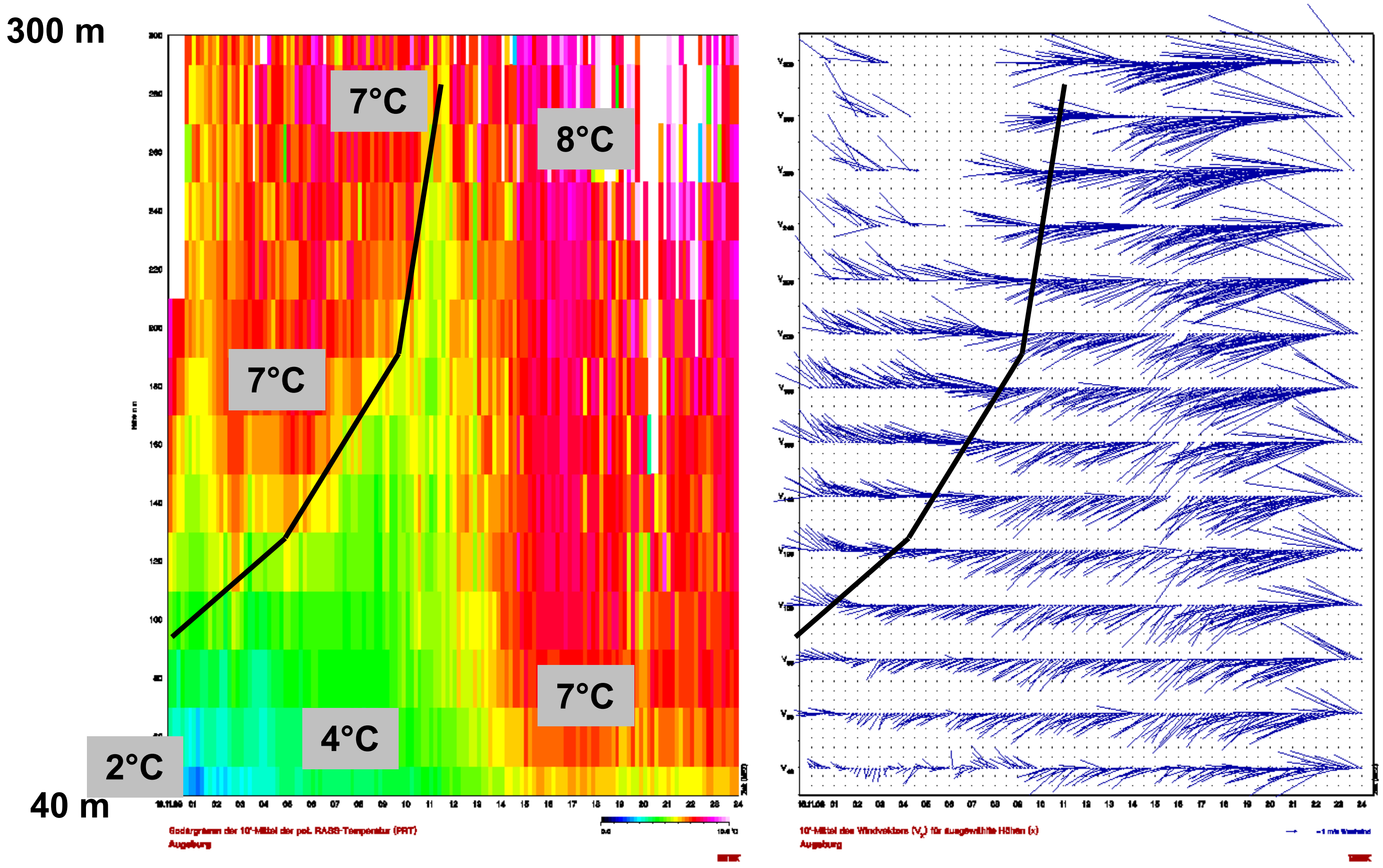

KIT – die Kooperation von
Forschungszentrum Karlsruhe GmbH
und Universität Karlsruhe (TH)

HELMHOLTZ GEMEINSCHAFT

Forschungszentrum Karlsruhe
in der Helmholtz-Gemeinschaft

Comparison of MLH retrievals with three different remote sensing techniques

SODAR
acoustic backscatter

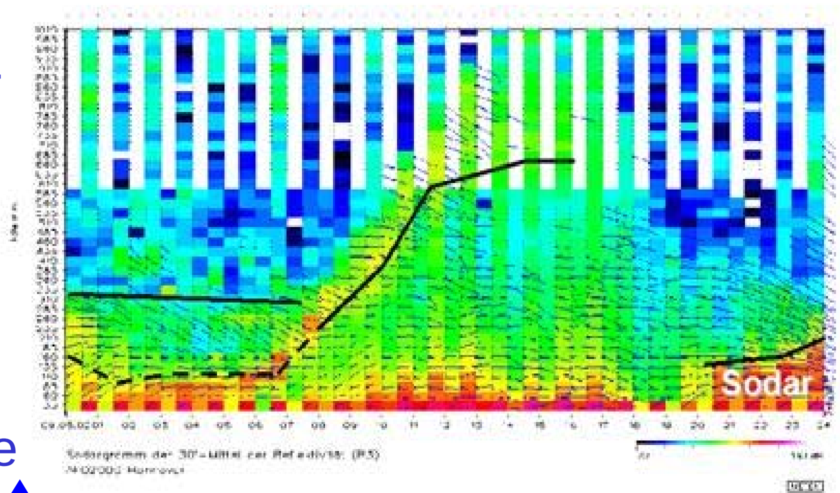

ceilometer
optical backscatter

RASS
temperature

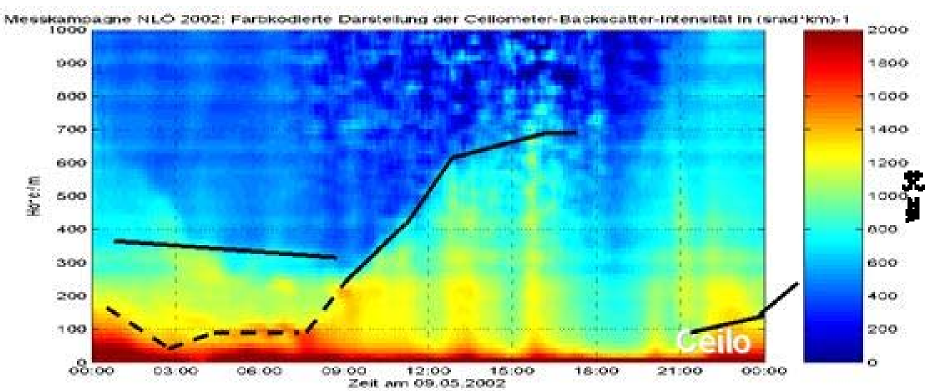

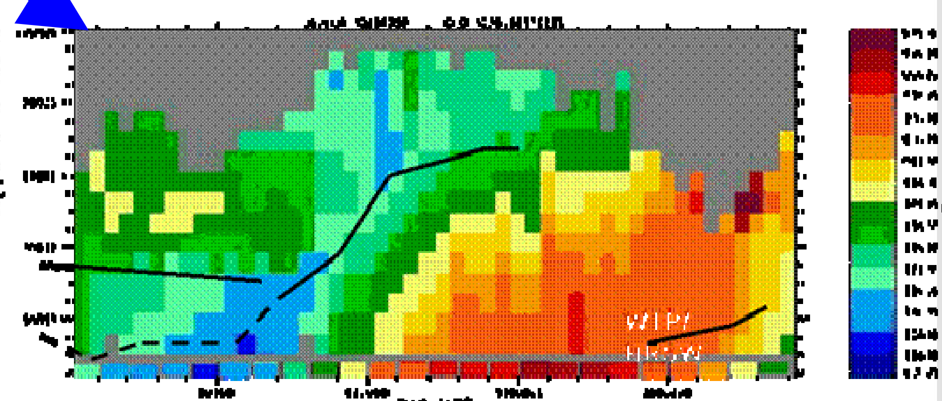

Emeis, S., Chr. Münkel, S. Vogt, W.J. Müller, K. Schäfer, 2004: Atmospheric boundary-layer structure from simultaneous SODAR, RASS, and ceilometer measurements. Atmos. Environ., 38, 273-286.

Summary

Overview on methods using ground-based remote sensing for the derivation of the mixing-layer height

method	short description
acoustic ARE method	analysis of **a**coustic **r**eceived **e**cho intensity profiles
" HWS method	analysis of **h**orizontal **w**ind **s**peed profiles
" VWV method	analysis of **v**ertical **w**ind **v**ariance profiles
" EARE method	analysis of acoustic backscatter intensity and vertical wind variance profiles (**e**nhanced **a**coustic **r**eceived **e**cho method)
optical threshold method	detection of a given backscatter intensity threshold
" gradient method	analysis of optical backscatter intensity profiles
" idealised backscatter method	analysis of optical backscatter intensity profiles
" wavelet method	analysis of optical backscatter intensity profiles
" variance method	analysis of optical backscatter intensity profiles
acoustic / electro-magnetic	ARE method applied to sodar and wind profiler data
acoustic / optical	EARE method plus gradient method
electro-magnetic / electro-magnetic	combination of a sodar-RASS and a wind profiler RASS: analysis of the vertical temperature profile plus analysis of the electro-magnetic backscatter intensity profile
acoustic / in situ	ARE method plus in-situ surface flux measurement

RASS	analysis of the temperature profile from the measured speed of sound

Conclusions:

**RASS directly delivers temperature profiles,
MLH, inversions, and stable layers can easily be detected,
wind profiles are additionally available.
Does not work properly under high wind speeds.**

**SODAR detects temperature fluctuations and gradients,
but no absolute temperature. Inversions and stable layers can indirectly be inferred with a MLH algorithm.
Does not work properly under perfectly neutral stratification, with very high wind speeds, and during stronger precipitation events.**

**Ceilometer detects aerosol distribution and water droplets. It has to be assumed that the aerosol follows the thermal structure of the atmosphere. Inversions and MLH can indirectly be inferred with a MLH algorithm.
Does not work properly in extreme clear (aerosol-free) air and during precipitation events and fog.**

Literature

SODAR:

Asimakopoulos, D.N., C.G. Helmis, J. Michopoulos, 2004: Evaluation of SODAR methods for the determination of the atmospheric boundary layer mixing height. - Meteor. Atmos. Phys. 85, 85–92.

Beyrich, F., 1997: Mixing height estimation from sodar data – a critical discussion. - Atmos. Environ. 31, 3941–3953.

Ceilometer:

Schäfer, K., S.M. Emeis, A. Rauch, C. Münkel, S. Vogt, 2004: Determination of mixing-layer heights from ceilometer data. In: Remote Sensing of Clouds and the Atmosphere IX. Schäfer, K., A. Comeron, M. Carleer, R.H. Picard, N. Sifakis (Eds.), Proc. SPIE, Bellingham, WA, USA, Vol. 5571, 248–259.

Sicard, M., C. Pérez, F. Rocadenbosch, J.M. Baldasano, D. García-Vizcaino, 2006: Mixed-Layer Depth Determination in the Barcelona Coastal Area From Regular Lidar Measurements: Methods, Results and Limitations. - Bound.-Lay. Meteor. 119, 135–157.

RASS:

Engelbart, D.A.M., J. Bange, 2002: Determination of boundary-layer parameters using wind profiler/RASS and sodar/RASS in the frame of the LITFASS project. Theor. Appl. Climatol. 73, 53–65.

Emeis, S., K. Schäfer, C. Münkel, 2009: Observation of the structure of the urban boundary layer with different ceilometers and validation by RASS data. Meteorol. Z., 18, 149-154. (Open access, freely available from http://dx.doi.org/10.1127/0941-2948/2009/0365)

Reviews:

Emeis, S., K. Schäfer, C. Münkel, 2008: Surface-based remote sensing of the mixing-layer height – a review. - Meteorol. Z., 17, 621-630. (Open access, freely available from http://dx.doi.org/10.1127/0941-2948/2008/0312)

Emeis, S., M. Harris, R.M. Banta, 2007: Boundary-layer anemometry by optical remote sensing for wind energy applications. - Meteorol. Z., 16, 337-347.